(19) Europäisches Patentamt
European Patent Office
Office européen des brevets

(11) EP 2 874 177 A1

(12) EUROPEAN PATENT APPLICATION

(43) Date of publication:
20.05.2015 Bulletin 2015/21

(51) Int Cl.:
H01J 49/00 *(2006.01)*

(21) Application number: **13306552.4**

(22) Date of filing: **13.11.2013**

(84) Designated Contracting States:
AL AT BE BG CH CY CZ DE DK EE ES FI FR GB GR HR HU IE IS IT LI LT LU LV MC MK MT NL NO PL PT RO RS SE SI SK SM TR
Designated Extension States:
BA ME

(71) Applicants:
- **Institut De Physique Du Globe De Paris (Établissement Public À Caractère Scientifique Et Technologique)**
  75005 Paris (FR)
- **Centre National de la Recherche Scientifique (CNRS)**
  75016 Paris (FR)

(72) Inventors:
- **Gourgiotis, Alkiviadis**
  75014 Paris (FR)
- **Louvat, Pascale**
  92500 Rueil-Malmaison (FR)
- **Moureau, Julien**
  75013 Paris (FR)
- **Gaillardet, Jérôme**
  93160 Noisy Le Grand (FR)

(74) Representative: **Regimbeau**
20, rue de Chazelles
75847 Paris Cedex 17 (FR)

(54) Method for correcting a drift of an isotopic ratio derived from data measured by a multi-collector mass spectrometer

(57) The invention relates to a method allowing the synchronization of the Faraday-amplifier signal responses in order to correct a drift of an isotopic ratio in a sample, on the basis of a first signal (Ia(t)) and a second signal (Ib(t)) derived from data measured by a multi-collector mass spectrometer (MC-ICPMS, MC-TIMS, IRMS), the first signal representing a variation of a detected quantity of a first isotope in the sample as a function of time, and the second signal representing a variation of a detected quantity of a second isotope in the sample as a function of time, said method comprising steps of:

- applying to the second signal a time offset (Δt) so as to obtain a second offset signal ($Ib(t+\Delta t)$),
- computing values of isotopic ratio between the first signal and the second offset signal at a plurality of times,
- computing an isotopic ratio variation parameter as a function of the computed values of isotopic ratio,
- adjusting the time offset (Δt) applied to the second signal and repeating the preceding steps so as to determine a time offset (Δt_{min}) for which the isotopic ratio variation parameter is reduced.

FIG. 3B

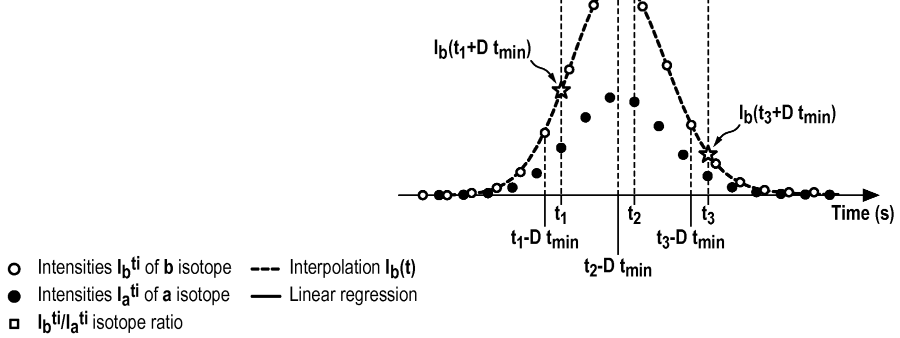

Printed by Jouve, 75001 PARIS (FR)

Description

FIELD OF THE INVENTION

[0001] The invention relates to a method for correcting a drift of an isotopic ratio derived from data measured by a multi-collector mass spectrometer.

BACKGROUND ART

[0002] Evaluation of isotopic ratios of a given element is an important source of information on the origin and transformation of a material. Isotopic analysis plays a leading part in the nuclear industry. It is also used in numerous fields, such as biochemistry, pharmacology, environment monitoring, criminal or food fraud fighting, geochemistry or cosmochemistry.

[0003] Measurement of isotopic ratios in a chemical element is generally made by mass spectrometry. Suitable instruments for these measurements are MC-ICPMS spectrometers (Multi Collector Inductively Coupled Plasma Mass Spectrometry) because of their low limit of detection, their high ionization potential, and simultaneous isotope analysis. These instruments offer isotopic ratio measurements on a large range of elements.

[0004] In order to eliminate possible isobaric interferences due to different elements having similar atomic masses in a sample, the sample to be measured should be treated by a separation technique before being introduced into the MC-ICPMS spectrometer. To that end, the MC-ICPMS spectrometer can be coupled with a variety of introduction systems which usually are: High Performance Liquid Chromatography (HPLC), Ion Chromatography (IC), Gas Chromatography (GC), Gold Trap (GT), Capillary Electrophoresis (CE) or IsoTachoPhoresis (ITP).

[0005] For *in situ* micro-analysis of solids or single micrometric particle size analysis, the MC-ICPMS can also be coupled with the Laser Ablation technique (LA).

[0006] Online coupling between these sample introduction systems and the MC-ICPMS spectrometer provides transient signals with specific time windows generally varying between some milliseconds to minutes in which the isotope ratios should be accurately measured.

[0007] However, most experiments reveal a systematic increase or decrease of the point by point isotope ratio during the transient signal, also called "isotopic ratio drift". Most commonly used methods for the isotope ratio calculation on transient signal (point by point method, linear regression method and Peak Area Integration method) do not correct this isotope ratio drift which significantly degrades the quality (i.e. repeatability and trueness) of the obtained measurements. According to the point by point method, the isotope ratio is determined for several points of a selected peak area centered around the maximum of the peak. The area of calculation is selected based on the stability of the measured isotope ratio. According to the linear regression method, the isotope ratio is given by the slope of the linear regression line which is the best fitting line through the data points obtained by plotting the signal intensities of the two isotopes as a function of one another. According to the Peak Area Integration method, the isotope ratio is obtained by dividing the integrated peak areas for the two isotopes.

[0008] For explaining the origin of this drift, one hypothesis is that the isotopic ratios derived from rapidly rising or decreasing signals are affected by responses of the mass spectrometer Faraday amplifiers. Depending on which amplifiers are faster or slower, measured signals become enhanced or reduced relative to each other.

[0009] In order to try to solve this problem, spectrometer constructors generally provide a calibration technique allowing the user to adjust *tau*-correction required for each of the Faraday amplifiers. Signal decay curves must first be empirically determined for each Faraday amplifier and then applied to remove residual bias resulting from prior signal variations from the individual readings.

[0010] However, such a calibration technique is generally not sufficient to completely remove the isotopic ratio drift. Even after *tau*-correction, time response of the different Faraday-amplifier systems may not be perfectly uniform and remaining isotope ratio drift in transient signals may be observed.

[0011] These remaining isotope ratio time variations could be attributed to residual capacities of the Faraday-amplifier systems due to the instrumental setup, the length and the geometry of the wiring between the collectors. These residual capacities called stray capacities can cause a lowering of the amplification system response and can vary among the individual Faraday-amplifiers.

[0012] There is thus a need for a method allowing the synchronization of the Faraday-amplifier signal responses providing an efficient correction of the isotopic ratio drift, also capable to enhancing repeatability or reducing uncertainty of isotopic ratio analysis. Such advantages can be of utmost importance when samples are in such quantities that only few analyses are allowed.

SUMMARY OF THE INVENTION

[0013] One aim of the invention is to provide an efficient method for correcting the drift of an isotopic ratio measured by a multi-collector mass spectrometer.

[0014] To that aim, the invention provides a method for correcting a drift of an isotopic ratio in a sample, on the basis of a first signal and a second signal derived from data measured by a multi-collector mass spectrometer, the first signal representing a variation of a detected quantity of a first isotope in the sample as a function of time, and the second signal representing a variation of a detected quantity of a second isotope in the sample as a function of time, said method comprising steps of:

- applying to the second signal a time offset so as to obtain a second offset signal,
- computing values of isotopic ratio between the first signal and the second offset signal at a plurality of times,
- computing an isotopic ratio variation parameter as a function of the computed values of isotopic ratio,
- adjusting the time offset applied to the second signal and repeating the preceding steps so as to determine a time offset for which the isotopic ratio variation parameter is reduced.

[0015] Introduction of a time offset allows adjusting the electronic hysteresis between the different amplifiers of the mass spectrometer. Such an adjustment is made after acquisition of the data and thus, does not require preliminary calibration of the mass spectrometer (i.e. technique for compensating the signal decay in the Faraday-amplifiers called "*tau*-correction").

[0016] The proposed method allows quantifying and correcting precisely the time offset between the different signals generated by the different amplifiers of the mass spectrometer, and thus provides an efficient correction of the isotopic ratios.

[0017] Moreover, the method uses the isotopic ratios between two signals, and not the intensity signal of each isotope independently. This allows a very precise calculation of the time offset and therefore, a fine correction of the isotopic ratio drift.

[0018] The method can be applied to each additional data, taking into account their specificity (such as the slope of the increase and decrease of the signal and the duration of the transient signal), as well as the variability of the hysteresis which may possibly vary between the different spectra (for instance depending on the intensity of the measured signals).

[0019] The proposed method can comprise a step of:

- computing the second signal by interpolation of second data representing detected quantities of a second isotope, measured in the sample at different times.

[0020] In particular, the interpolation can be a piecewise polynomial interpolation, preferably a third degree piecewise polynomial interpolation.

[0021] The steps of the method can be applied to a number N of signals, N>2, each i-th signal representing a variation of a detected quantity of a i-th isotope in the sample as a function of time, so as to determine a time offset for each of the second to the N-th signals.

[0022] According to a first embodiment of the invention, the isotopic ratio variation parameter is a slope as a function of time of a straight line obtained by linear regression of the values of isotopic ratio.

[0023] According to a second embodiment of the invention, the isotopic ratio variation parameter is a relative standard deviation of the isotopic ratio values.

[0024] The method can comprise a step of:

- selecting a time interval in which the values of isotopic ratio are computed.

[0025] The steps can be carried out on several time intervals, and a time offset is determined for each time interval.

[0026] The proposed method can comprise preliminary steps of:

- introducing a sample into the multi-collector mass spectrometer, and
- measuring data from the sample, the data being measured by the spectrometer.

[0027] In particular, the multi-collector mass spectrometer is coupled to an ion source. Such an ion source may be selected from the group consisting in a thermal ionization device, an electron ionization device and a plasma ionization device. In a preferred embodiment, the ion source is an inductively coupled plasma device. Hence, in a more preferred embodiment, methods of the invention can be applied to data measured by a multi-collector inductively coupled plasma mass spectrometer (MC-ICPMS), a multi-collector thermal ionization mass spectrometer (MC-TIMS) or an Isotopic Ratio mass spectrometer (IRMS).

[0028] In particular, the multi-collector mass spectrometer may be coupled to a separation system for separating the sample into several elementary fractions and successively introducing the elementary fractions into the spectrometer.

[0029] Such a separation system may be a liquid chromatography, high performance liquid chromatography, ion chromatography, gas chromatography, gold trap, capillary electrophoresis or isotachophoresis.

[0030] Alternately, for *in situ* isotope analysis the multi-collector mass spectrometer can also be coupled to a Laser Ablation (LA) system and for low sample volumes analysis to a flow injection (FI) system.

PRESENTATION OF THE DRAWINGS

[0031] The invention will be described with reference to the drawings, in which:

- Figure 1 diagrammatically shows a multi-collector mass spectrometer comprising a data collection and processing unit programmed for carrying out a method for correcting a drift of an isotopic ratio, according to a possible embodiment of the invention,
- Figure 2 diagrammatically shows different steps of the method for correcting a drift of an isotopic ratio,
- Figures 3A and 3B diagrammatically shows transient signals I_a(ti) and I_b(ti) of a given element X, and a linear positive drift of the isotopic ratio when no correction is applied (Figure 3A), and the isotopic ratio when a correction is applied (Figure 3B),
- Figures 4A to 4C respectively show the linear increasing of values of the isotopic ratio ^{208}Pb/^{206}Pb measured point-by-point (Figure 4A), values of the isotopic ratio ^{208}Pb/^{206}Pb after correction with a method according to the invention (Figure 4B), and a comparison of the first embodiment of the method based on the slope obtained by linear regression of the values of isotopic ratio and the second embodiment of the method based on a relative standard deviation of the values of isotopic ratio (Figure 4C), wherein data were acquired using flow injection and demountable direct injection high efficiency nebulizer (d-DIHEN) in the Neptune MC-ICPMS,
- Figures 5A to 5D respectively show Pb transient signals acquired using flow injection and d-DIHEN in the Neptune MC-ICPMS with an integration time (it) of 0.262 seconds (Figure 5A), corresponding time corrected isotope ratios (Figure 5B), Pb transient signals acquired with an integration time of 1.049 seconds (Figure 5C) and corresponding time corrected isotope ratio (Figure 5D),
- Figures 6A to 6D respectively show a Pb transient signal acquired using a GC directly coupled with a Nu MC-ICPMS and isotope ratios before and after drift correction of: ^{208}Pb/^{206}Pb (Figure 6A), ^{207}Pb/^{206}Pb (Figure 6B) and ^{204}Pb/^{206}Pb (Figure 6C), as well as slope values before (S_b) and after (S_a) isotope ratio drift correction, and Δt_{min} values for the *Slope* and *RSD* models for the ^{208}Pb/^{206}Pb, ^{207}Pb/^{206}Pb and ^{204}Pb/^{206}Pb isotope ratios (Figure 6D),
- Figures 7A to 7D respectively show three isotope plots for the GC-MC-ICPMS: ^{208}Pb/^{206}Pb versus ^{207}Pb/^{206}Pb (Figure 7A) and ^{208}Pb/^{206}Pb versus ^{204}Pb/^{206}Pb (Figure 7B), and point by point percentage relative deviations from the Exponential Mass Fractionation Law for a given ^{208}Pb/^{206}Pb ratio of: ^{207}Pb/^{206}Pb (Figure 7C) and ^{204}Pb/^{206}Pb (Figure 7D),
- Figures 8A and 8B show blank-corrected and mass fractionation-corrected ^{207}Pb/^{206}Pb (Figure 8A) and ^{204}Pb/^{206}Pb (Figure 8B) isotope ratios of GC-MC-ICPMS thirty injections, all data having been treated before and after isotope ratio drift correction with Point by Point (PbP), Linear Regression (LR) and Peak Area Integration (PAI) methods.

DETAILLED DESCRIPTION OF AN EMBODIMENT OF THE INVENTION

[0032] Referring to figure 1, the multi-collector mass spectrometer comprises a control unit 1, a separation and/or an injection system 2, an ion source 3, a magnetic sector 4, a multi-collector array 5 and a data collection and processing unit 6.

[0033] The control unit 1 is capable of controlling hardware and software components of the mass spectrometer. Such a control unit 1 may be a computer. The separation and/or an injection system 2 is a device which introduces a small amount of sample into the ion source 3 through an inlet. The ion source 3 is used for converting a portion of the sample into charged particles such as atomic ions. Such an ion source may be a plasma source, a gas source or a thermal ionization source. The magnetic sector 4 allows the separation of the ions by charge to mass ratios. The multi-collector array 5 is a ion collector, typically having an array of detector-amplifiers (or Faraday cups), which allows simultaneous detection of multiple isotopes. The data collection and processing unit 6 is configured to process and store data measured by the multi-collector array. It can comprise a computer for processing the data and a storage unit for storing the measured and processed data. Moreover, the data collection and processing unit 6 is programmed for correcting a drift of an isotopic ratio in the sample according to a possible embodiment of the method for correcting the drift of an isotopic ratio.

[0034] Chemical components which may be subjected to isotopic ratio measurements comprise rare earth elements, alkaline earth metals, transition metals and actinides.

[0035] Referring to figure 2, different steps of a method 100 for correcting a drift of an isotopic ratio are illustrated.

[0036] According to a first step 101, a sample is introduced into a multi-collector mass spectrometer (MC-MS).

[0037] To that end, the multi-collector mass spectrometer may be coupled to a separation system, such as a liquid or a gas chromatography system, a Gold Trap (GT), a Capillary Electrophoresis (CE) or a IsoTachoPhoresis (ITP) for separating the sample into several elementary fractions and successively introducing the elementary fractions into the spectrometer.

[0038] In case the material to be tested is a solid, the multi-collector mass spectrometer may be coupled to a laser ablation system for *in situ* analysis, or to a flow injection system for low volume sample analysis.

[0039] The multi-collector mass spectrometer comprises several detector-amplifier systems, each detector-amplifier being configured to measure a quantity of a given isotope in the sample.

[0040] According to a second step 102, data from the sample are acquired by the detector-amplifier systems of the mass spectrometer. The acquired data may comprise data measured for a number N of isotopes in the sample ($N \geq 2$).

[0041] In the example illustrated, on figure 2, data are measured for two isotopes a and b.

[0042] The acquired data comprises first data and second data.

[0043] The first data comprise quantities of a first isotope (isotope a) measured by a first detector-amplifier system at different times.

[0044] The second data comprise quantities of a second isotope (isotope b) measured by a second detector-amplifier system at different times.

[0045] Figure 3A shows an example of first data (I_a) for the isotope a, second data (I_b) for the isotope b, and values of isotopic ratio I_b/I_a of an element X at the different times t_i.

[0046] The acquired data are processed by the data collection and processing unit which may be part of the mass spectrometer or may be separated from the mass spectrometer. The data collection and processing unit is programmed for applying subsequent steps of the method.

[0047] A first signal I_a is defined as being the first data representing detected quantities of the first isotope a, measured in the sample at different times t_i. The first signal is thus composed of discrete measurement results with their associated timestamp reads.

[0048] According to a third step 103, the data collection and processing unit computes a second signal I_b by interpolation of second data representing detected quantities of a second isotope (b), measured in the sample at different times.

[0049] Preferably, the second signal $I_b(t)$ is computed by piecewise polynomial interpolation of the second data representing detected quantities of the second isotope b, measured in the sample at different times t_i.

[0050] According to such piecewise polynomial interpolation, a series of third polynomial curves through the successive points of the data (i.e. piecewise) is interpolated, which permits to create a well-behaved curve (no oscillations that are not supported by the data) rather than to generate a single polynomial.

[0051] The third interpolation order is preferred because it is the lowest order polynomial for which curvature can be continuous. Lower order polynomials can be used but the result may be a jagged curve if there are many changes in slope.

[0052] Figure 3B shows an example of a second signal $I_b(t_i)$ together with its interpolated curve $I_b(t)$ and corresponding values of drift corrected isotope ratio I_b/I_a of an element X at different times t_i.

[0053] According to a fourth step 104, a time interval is selected in which a correction is to be applied.

[0054] To that end, the data collection and processing unit may display a diagram showing first and second signals $I_a(t)$ and $I_b(t)$, so that the user may select a time interval.

[0055] Alternatively, the data collection and processing unit may select automatically an appropriate time interval.

[0056] Additionally, the selection can be performed several times at several stages of the method.

[0057] As illustrated on figure 3A, an example of selected time interval is $[t_1, t_3]$.

[0058] Within this time interval, the variation of the isotope ratio I_b/I_a as a function of time may be modeled by a linear function having a slope S defined by:

$$S = \frac{\sum_{i=1}^{n}\left(\frac{I_b(t_i)}{I_a(t_i)}\right) \times \sum_{i=1}^{n} t_i - n \times \sum_{i=1}^{n}\left(t_i \cdot \frac{I_b(t_i)}{I_a(t_i)}\right)}{\left(\sum_{i=1}^{n} t_i\right)^2 - n \times \sum_{i=1}^{n} {t_i}^2} \qquad [1]$$

where n is the number of isotope ratio values for computing the slope S, and t_i are the timestamp read.

[0059] Optionally, a reunion of several time intervals can be selected.

[0060] According to a fifth step 105, the data-collection and processing unit applies a time offset Δt to one of the signals computed by interpolation, typically the second signal according to the embodiment described and illustrated, so as to obtain a second offset signal ($I_b(t+\Delta t)$).

[0061] In the case of several time intervals, a time offset can be determined for each time interval, the time offset being possibly different from one time interval to another.

[0062] According to a sixth step 106, the data collection and processing unit computes values of isotopic ratio, from the first signal $I_a(t)$ and the second offset signal $I_b(t+\Delta t)$ at a plurality of times t_i within the time interval.

[0063] For a given time t_i, the isotopic ratio is computed as a ratio of the intensity of the second signal $I_b(t_i+\Delta t)$ on the intensity of the first signal $I_a(t_i)$. Alternatively, the isotopic ratio could be calculated as a ratio of the intensity of the first signal $I_a(t_i+\Delta t)$ on the intensity of the second signal $I_b(t_i)$. Alternatively, the isotopic ratio could be calculated as a ratio of the intensity of the first signal $I_a(t_i)$ on the intensity of the second signal $I_b(t_i+\Delta t)$.

[0064] According to a seventh step 107, the data collection and processing unit computes an isotopic ratio variation parameter as a function of the values of isotopic ratios computed during the fifth step 106.

[0065] Steps 105 and 106 can typically be performed during step 107.

[0066] The isotopic ratio variation parameter is preferably chosen so as to be easily computed. The isotopic ratio is typically chosen so as to avoid highly divergent isotope ratio values, for instance by an adapted normalization.

[0067] According to a first embodiment, the isotopic ratio variation parameter includes the absolute value of the slope S of a straight line obtained by linear regression of isotopic ratio values.

[0068] An example of such an isotopic ratio variation parameter is typically defined as follows by formula [2]:

$$|S(\Delta t)| = \left| \frac{\sum_{i=1}^{n}\left(\frac{I_b(t_i+\Delta t)}{I_a(t_i)}\right) \times \sum_{i=1}^{n} t_i - n \times \sum_{i=1}^{n}\left(t_i \cdot \frac{I_b(t_i+\Delta t)}{I_a(t_i)}\right)}{\left(\sum_{i=1}^{n} t_i\right)^2 - n \times \sum_{i=1}^{n} {t_i}^2} \right| \qquad [2]$$

where Δt is the time offset applied to the second signal and n is the number of isotope ratio values for computing the slope S.

[0069] According to a second embodiment of the invention, the isotopic ratio variation parameter includes a relative standard deviation of the values of isotopic ratio.

[0070] An example of such an isotopic ratio variation parameter is typically is defined as follows by formula [3]:

$$RSD(\Delta t) = \left(\frac{\sqrt{\frac{\sum_{i=1}^{n}\left(\frac{I_b(t_i+\Delta t)}{I_a(t_i)} - \frac{1}{n} \cdot \frac{\sum_{i=1}^{n} I_b(t_i+\Delta t)}{I_a(t_i)}\right)^2}{n-1}}}{\frac{1}{n} \cdot \sum_{i=1}^{n} \frac{I_b(t_i+\Delta t)}{I_a(t_i)}} \right) \times 100 \qquad [3]$$

where Δt is the time offset applied to the second signal and n is the number of isotope ratio values for computing the relative standard deviation RSD.

[0071] Alternatively, the isotopic ratio variation parameter can be a combination of both first a second embodiments.

[0072] The slope-model according to the first embodiment can only be used if a systematic increase or decrease of the isotopic ratio with time is observed.

[0073] In the case of fast random changes of the isotopic ratio with time due to noisy or spiky signal behavior, the RSD-model according to the second embodiment is more appropriate for use.

[0074] According to an eighth step 108, the data collection and processing unit adjusts the time offset Δt applied to the second signal so as to determine a time offset (Δt_{min}) for which the isotopic ratio variation parameter is reduced.

[0075] Accordingly, the eighth step 108 can include a modification of the value of the time offset Δt. The eighth step 108 can then include that the data collection and processing unit repeats steps 105 to 107 with the new time offset.

[0076] According to the first embodiment, the adjustment step is performed until the slope S is null or inferior to a predetermined value. For example, the data collection and processing unit repeats steps 105 to 108 until the slope S is null or inferior to 10^{-7}. Typical slope values after Δt adjustment range from 10^{-10} to 10^{-16} (isotope ratio/second).

[0077] According to the second embodiment, the adjustment step is performed until the relative standard deviation RSD raises a minimum or at least has decreased to a value that is estimated to be close enough to a minimum. For example, the data collection and processing unit repeats steps 105 to 108 until the relative standard deviation RSD raises a minimum or at least has decreased to a value that is estimated to be close enough to a minimum.

[0078] The time offset Δt_{min} is obtained when isotopic ratio variation parameter raises a minimum or is estimated to be close enough to a minimum.

[0079] Both isotopic ratio variation parameter (slope S and relative standard deviation RSD) lead to very similar values of time offset Δt_{min}. However, the slope-based model is only applicable when a monotonic drift is observed. The relative standard deviation model may be applied in all cases, even in case of rapid and random variation of the isotopic ratio, which can be observed when coupling the mass spectrometer to a laser ablation system.

[0080] Such a time offset Δt_{min} is applied to the second signal I_b so as to correct the drift in the isotopic ratio I_b/I_a. The method allows computing corrected isotopic ratio values, free from artifacts caused by detection and amplification systems of the spectrometer.

[0081] The time corrected isotopic ratio values are typically defined by formula 4 as follows:

$$\frac{I_b(t_i + \Delta t_{min})}{I_a(t_i)} \qquad [4]$$

[0082] In case of N isotopes in the sample ($N \geq 2$), the same method is applied to the data measured for the i-th isotope. A time offset Δt_{min} is determined for each i-th signal taking one of the signals, for instance the first signal I_a, as a reference signal.

[0083] According to a ninth step 109, the data collection and processing unit computes a final value of isotopic ratio as a function of the first signal $I_a(t_i)$ and of the second corrected signal $I_b(t_i+\Delta t_{min})$.

[0084] Several methods can be used to compute the final value of isotopic ratio.

[0085] An average peak method can be applied, wherein the final value of isotopic ratio is computed as a mean value of the time corrected isotopic ratio values, within a selected time interval, which can be the same as or different from the time interval selected at step 104.

[0086] Alternatively, a linear-regression slope method can be applied, wherein a linear regression of the first signal $I_a(t)$ as a function of the second corrected signal $I_b(t+\Delta t_{min})$ is computed, and the final value of isotopic ratio is calculated as the slope of the straight line obtained by the linear regression.

[0087] After isotope ratio drift correction both methods give similar results.

EXAMPLE 1: Transient signals with direct injection as introduction system

[0088] The Neptune MC-ICPMS (ThermoFinnigan, Germany) used in this example is equipped with a multicollector system with nine Faraday cups attached to 10^{11} Ohms resistors (dynamic range from 0 Volt to 50 Volts) for simultaneous detection and provides high mass-resolution capabilities. All measurements were performed in static multicollection mode with Faraday cups. The Faraday-amplifier gains were calibrated daily before the analytical session yielding a reproducibility of the electric gains better than 10 ppm per day. Faraday-amplifier systems have been corrected for compensation of signal decay (*tau*-correction) according to the procedure recommended by the constructor. Intensities at m/z=202 were monitored for eventual ^{204}Hg isobaric interference corrections and found to be inferiors to 0.1milliVolts. All samples were injected into the plasma through a demountable direct injection high efficiency nebulizer (d-DIHEN) directly coupled to a flow injection system. The flow injection system consists of a six-way high flow valve (ESI FAST) with an injection loop of 5 μL and a peristaltic pump which ensure the continuous flow of the carrier solution (HNO_3, 0.5N). Cup configuration for Pb measurements and MC-ICPMS operating conditions are summarized in Table 1.

[0089] All sample dilutions were performed with 0.5 M nitric acid obtained from sub-boiled 14 M nitric acid (EVAPOCLEAN system, Analab, France) and deionised water (Milli Q system, Millipore, Milford, MA, USA). The same acid was also used as the carrier solution for the flow injection. For all Pb injections (Neptune-dDIHEN, Nu-GC) the SRM981 standard solution was used and all calculations were performed by taking into account the isotopic composition as was reevaluated by Doucelance and Manhès (Doucelance, R.; Manhès, G. Chemical Geology 2001, 176, 361-377):$^{208}Pb/^{206}Pb$ = 2.1681, $^{207}Pb/^{206}Pb$ = 0.914970(17), $^{204}Pb/^{206}Pb$ = 0.059019(5).

[0090] Pb transient signals were investigated after flow injection and using a demountable direct injection high efficiency nebulizer (d-DIHEN) as the introduction system in the Neptune MC-ICPMS. For this purpose, 5 μL of a 100 ppb SRM981 standard solution were pushed from the carrier solution into the torch. Although flow injection system has already been used for transient signal studies, the aim of the d-DIHEN is to eliminate as maximum as possible parameters like memory blanks and processes during generation and transportation of the aerosol from the spray chamber to the torch. The objective is therefore to minimize all external parameters which could induce an isotope ratio fractionation and to highlight isotope ratio drift due to the time lag between the Faraday-amplifier systems. For transient signal data acquisition an integration time (*it*=0.524 s) longer than the time constant of the Faraday preamplifier response (~0.1 s) was chosen.

[0091] The $^{208}Pb/^{206}Pb$, $^{207}Pb/^{206}Pb$ and $^{204}Pb/^{206}Pb$ isotope ratios were investigated and only the $^{208}Pb/^{206}Pb$ ratio showed a significant drift. As can be seen in Figure 4A the point by point $^{208}Pb/^{206}Pb$ isotope ratio shows a systematic increase with time (~0.15%) over a period of ~20 s, which is significantly longer than the time constant of the Faraday-amplifier system. Therefore, this drift can be attributed to the time lag between H1/H3 (Table 1) Faraday-amplifier systems.

[0092] For the isotope drift correction the blank-corrected ^{208}Pb and ^{206}Pb intensities with their respective timestamp reads as were recorded from the onboard computer were used. Blank intensities were calculated for each isotope as the average value of a time window prior transient signal peak. Before model use, data processing involves the blank subtraction from each intensity point of ^{208}Pb and ^{206}Pb isotopes. ^{206}Pb isotope is considered as the reference system and timestamp and intensity reads of ^{208}Pb were used for obtaining the intensity function $I_{208}(t)$ by the Piecewise Polynomial Interpolation (PPI) method. In order to be able to efficiently calculate the time lag (Δt_{min}) between H1 and H3 Faraday-amplifiers, the two models were applied in a specific time-zone where isotope ratio shows a steady trend avoiding high isotope ratio noisy or spiky behavior (Figure 4A, zone taken into account for the linear regression). This zone corresponds to ^{208}Pb intensities higher than ~2 Volts. A graphical visualization of the models behavior as a function of Δt is given in Figure 4B. As can be seen, Δt_{min} for the *RSD* model is slightly shifted toward lower time values compared to the minimum of the *Slope* model. Indeed, after *Slope* and *RSD* models minimization, Δt_{min} values have found to be equal to 0.00165 s and 0.00154 s respectively. Nevertheless, the *Slope* model presents a sharp shape in the minimum region whereas the *RSD* model shows a quasi-invariant profile for the same region. Consequently, for Δt = 0.00165 s, the *RSD* model is equal to 0.019785 which is not significantly different compared to the RSD_{min} value equal to 0.019725 (obtained for Δt = 0.00154 s). Thus, it can be considered that Δt_{min} values obtained by models minimization are in good agreement with each other.

[0093] Through equation [5], the calculated time lag can approximately be expressed as the difference between the stray capacitances of H1 and H3 collector systems which is called relative stray capacitance.

$$\tau + \Delta t_{min} = R(C + \Delta C) \qquad [5]$$

where τ, *R*, *C*, are the time constant, the resistor and the capacitor of the Faraday collector system, ΔC is denoted the relative stray capacitance between H1 and H3 collector systems, respectively.

[0094] For typical values of $R=10^{11}\ \Omega$, $C=10^{-12}$ F, τ=0.1 s and Δt_{min}=0.0016 s, ΔC was found to be equal to 0.016 pF. Therefore, a very small relative stray capacitance (0.016 pF) between H1 and H3 collector systems induce a time lag in the order of magnitude of ~0.0016 s which in turn induce a $^{208}Pb/^{206}Pb$ isotope ratio drift of ~1.5‰.

[0095] Then, the time corrected $^{208}Pb/^{206}Pb$ isotope ratio was calculated using equation [4] and the Δt_{min} value from the *Slope* model (Figure 4C). Values of the slope and standard deviation for the selected isotope ratio zone before and after models correction are given in Table 2. By comparing the slopes, it can be seen that model efficiently corrects the isotope ratio drift.

[0096] The influence of the signal integration time on the isotope ratio drift was also investigated. Two independent injections of Pb were performed with 0.262 seconds and 1.049 seconds integration times respectively. For injection with 0.524 seconds integration time, only the $^{208}Pb/^{206}Pb$ isotope ratios showed a significant time dependent drift (Figures 5A et 5C). As can be seen from Figures 4A, 5A et 5C, a similar trend of the $^{208}Pb/^{206}Pb$ isotope ratio drift for the three different integration times was observed. Moreover, the isotope ratio slopes calculated for the linear regression zones displayed similar values (Table 2, values of slope before model correction).

[0097] Therefore, it can be concluded that integration time has not a significant influence on the isotope ratio drift. In contrast, in the same figures it can be observed that higher integration times lead to smoother ^{208}Pb signal profiles and to smaller isotope ratio random variations. It should be noted that for transient signals with spiky and nosy shapes (i.e. laser ablation) the use of relatively long integration times compared to the signal variations (i.e. >0.2 s), could induce inaccurate tracking of the ion signals and consequently can influence the isotope ratio drift.

[0098] Δt_{min} values were then calculated by the application of the two models in the linear regression zones (Figures 5A and 5C) and were found to be in good agreement with Δt_{min} values for 0.524 s integration time. Furthermore, like 0.524 s integration time, Δt_{min} values obtained by the *RSD* model were found to be systematically slightly shifted toward lower time values compared to the Δt_{min} of the *Slope* model (Table 2). For isotope ratio time correction, the equation [4] and the Δt_{min} values of the *Slope* model were used (Figure 5B and 5D).

[0099] Isotope ratio drift correction also highlights the integration time influence on the % RSD calculated for the linear regression zones. Although higher integration times lead to smaller isotope ratio random variations, % RSD values before model correction are dominated by the isotope ratio drift and therefore changes of the integration time have no significant impact to the %RSD values. In contrast, after isotope ratio drift correction, it is clear that % RSD for 1.049 s is widely lower than that of 0.262 s (Table 2).

EXAMPLE 2: GC-MC-ICPMS coupling for Pb isotope ratio determination

[0100] The Nu Plasma HR MC-ICPMS (Nu instrument, Wrexham, U.K.) is equipped with twelve Faraday cups attached to 10^{11} Ω resistors for simultaneous detection (dynamic range from 0 V to 10 V). For Pb isotope ratio measurements, in order to increase the dynamic range of the H4 collector for ^{208}Pb detection, two preamplifiers were connected to the Faraday cup achieving 20 Volts dynamic range (from -10 V to 10 V). All measurements were performed in static multicollection mode with Faraday cups. Faraday-amplifier gains were calibrated daily before the analytical session yielding a reproducibility of the electric gains better than 10 ppm per day. Tau-correction was performed for all Faraday-amplifier systems. Correction for isobaric interference on mass 204 was unnecessary firstly because Hg is not present in the standard solution and secondly Hg species do not elute at the same time as $PbEt_4$. However, ^{204}Hg presence was monitored using ^{202}Hg and for all injections ^{202}Hg intensities have found to be inferiors to 0.1 milliVolts.

[0101] A commercially double-inlet torch was used for the Gas Chromatography (GC) hyphenation and the simultaneous introduction of Tl solution (200 μL min^{-1} of a 200 ng mL^{-1} solution) through a self-aspirating microconcentric nebulizer coupled to a cinnabar spray chamber. Instrumental operation conditions and cup configuration are summarized in Table 1.

[0102] The developed method for isotope ratio drift correction in transient signals was applied in data acquired by gas chromatography directly coupled to a Nu MC-ICPMS for Pb isotope ratio determination. These data consist of thirty independent injections of a NIST SRM981 standard solution. Data acquisition was performed in static multicollection mode with an integration time of 0.5 seconds. Elution Pb profiles were highly reproducible in time, peak-shape and maximum intensity. Typical isotope ratio profiles during Pb elution are given in Figures 6A to 6C. As can be seen the blank-corrected point by point isotope ratios showed a negative time drift for ^{208}Pb/^{206}Pb ratio (decrease with time, ~1.05%) and a positive drift for ^{207}Pb/^{206}Pb and ^{204}Pb/^{206}Pb ratios (increase with time, ~0.35% and ~0.17% respectively). Theoretically, in this case in which a GC issued as the MC-ICPMS introduction system, both chromatographic separation and time lag between the Faraday-amplifier systems can be considered as the source of the observed isotope ratio drift. The capillary GC column separates species by boiling point and thus separation would obey physical laws of isotope mass fractionation favoring the elution of light isotope masses. Therefore, if the major source of the observed isotope ratio drifts is mass dependent isotope fractionation in the GC column, ^{208}Pb/^{206}Pb and ^{204}Pb/^{206}Pb ratios should show a positive and negative drift respectively during Pb elution. Comparing this theoretical consideration with experimental results (Figure 6A and 6C), it is clear that GC mass fractionation cannot be the cause of this drift. Only ^{207}Pb/^{206}Pb isotope ratio drift is consistent with a possible isotope mass fraction in the GC column (Figure 6B). In order to shed more light on the source of this drift, the ^{204}Pb/^{206}Pb and ^{207}Pb/^{206}Pb isotope ratios were plotted against ^{208}Pb/^{206}Pb ratios and compared to the Exponential Mass Fractionation Low (EMFL). For these diagrams, the blank-corrected isotope ratios from the linear regression zones of the thirty injections were plotted together (Figure 7A and 7B).

[0103] If the observed drifts are caused by a mass-dependent fractionation in the GC column, the uncorrected data of Figures 7A and 7B should be in good agreement with the EMFL. Any statistically significant deviation from the EMFL is considered as a mass-independent fractionation. As can be seen, important deviations from the EMFL clearly point out that the major source of ^{204}Pb/^{206}Pb, ^{207}Pb/^{206}Pb and ^{208}Pb/^{206}Pb isotope ratio drifts cannot be the isotope mass-dependent fractionation in the GC column during Pb elution. However, due to the high degree of these deviations (~0.4%), their origin seems to come more from the instrument (MC-ICPMS) than processes like nuclear volume and nuclear spin traditionally responsible to mass-independent fractionations. Therefore, the time lag between the Faraday-amplifier systems is considered as the major source for explaining this unpredictable behavior of the isotope ratio drifts.

[0104] For the isotope ratio drift correction, the same procedure previously described for the d-DIHEN introduction system was used. The ^{206}Pb isotope is considered as the reference system and timestamp and intensity reads of ^{204}Pb, ^{207}Pb and ^{208}Pb isotopes were used for obtaining the intensity functions $I_{204}(t)$, $I_{207}(t)$ and $I_{208}(t)$ respectively.

[0105] For each injection, Δt_{min} was calculated by both *the Slope* model and the *RSD* model. The values were found to be in good agreement each other with Δt_{min} relative differences between the two models of <0.2%, <1% and <4% for the ^{208}Pb/^{206}Pb, ^{207}Pb/^{206}Pb and ^{204}Pb/^{206}Pb ratios respectively. The Δt_{min} values of both models and for the thirty injections are given in Figure 6D. As can be seen, Δt_{min} of ^{208}Pb/^{206}Pb and ^{207}Pb/^{206}Pb ratios have found to be reproducible with average values of -0.0076 $\pm$ 2.6% s (2σ) and 0.00269 $\pm$ 8.0% s (2σ) respectively. Negative time lag means that the H4 Faraday-amplifier system lags behind the H2 reference system (^{206}Pb isotope). Unlike other the isotope ratios, Δt_{min} values of the ^{204}Pb/^{206}Pb ratio showed high fluctuations between different injections with an average value equal to 0.00115 $\pm$ 74.6% s (2σ). The large time lag observed for the H4/H2 Faraday cups could be explained by the use of two amplifiers for increasing the dynamic range of the H4 collector.

[0106] It should be also noted that, even if time lag between the Faraday-amplifier systems is the dominant source of the observed isotope ratios drift, mass-dependent isotope fractionation in the GC column cannot be excluded. Column isotope fractionation generates an isotope ratio drift that should be added or subtracted to the drift originating from the

Faraday-amplifier time lag (addition for the same slope signs and subtraction otherwise).

[0107] For the isotope ratio time correction the Δt_{min} values obtained from the *Slope* model were used. When comparing the $^{204}Pb/^{206}Pb$, $^{207}Pb/^{206}Pb$ and $^{208}Pb/^{206}Pb$ slopes of the linear regressions before and after Δt_{min} correction, it appears that isotope ratio drift is efficiently corrected by the model (Figure 6A, 6B and 6C). Moreover, after drift correction the data much better fit the EMFL (Figure 7A and 7B).

[0108] The observed dispersion of the corrected data along the EMFL is due to instrumental mass fractionation changes during the different injection sessions. This is also confirmed by Tl which was continuously introduced into the torch without passing through GC column. Fractionation factors (β) of $^{205}Tl/^{203}Tl$ and $^{204}Pb/^{206}Pb$, $^{207}Pb/^{206}Pb$, $^{208}Pb/^{206}Pb$ ratios reveal identical variations.

$\Delta^{204}Pb/^{206}Pb$ and $\Delta^{207}Pb/^{206}Pb$ DIAGRAMS

[0109] In order to highlight small deviations of the drift corrected data from the EMFL (Figure 7A, 7B) at the level of some ppm, representations of $\Delta^{204}Pb/^{206}Pb$ and $\Delta\ ^{207}Pb/^{206}Pb$ against ^{208}Pb signal were used (Figure 7C and 7D). $\Delta^{204}Pb/^{206}Pb$ and $\Delta^{207}Pb/^{206}Pb$ correspond to the differences between measured and calculated ratios according to the reference EMFL for a given $^{208}Pb/^{206}Pb$ ratio. The ^{208}Pb signal intensity was used in the X-axis due to the continuously changing signal which significantly influences the counting statistics (Poisson law) and therefore the isotope ratio precision. As can be seen on Figure 7C, for ^{208}Pb intensities higher than 10 V, $^{207}Pb/^{206}Pb$ ratios show downward trend relative to the EMFL with an average value of about 250 ppm. In contrast, for intensities lower than 10 V, the data show a random dispersion around the EMFL. Different fractionation laws were also used (Power law and Linear Law) and displayed differences relative to the EMFL which are not distinguishable for the dispersion of our data. This isotopic deviation from the EMFL has been attributed to the superposition of the classical mass discrimination isotope evolution (EMFL) with a non-exponential effect whose physical origin has not been identified yet. Unlike $^{207}Pb/^{206}Pb$, $^{204}Pb/^{206}Pb$ results are not conclusive due to the high point dispersion around the EMFL (Figure 7B).

UNCERTAINTIES OF INDIVIDUAL INJECTIONS, REPEATABILITY AND TRUENESS

[0110] The performances of the drift correction on the isotope ratio uncertainty, trueness and repeatability were also tested and evaluated. The data of the thirty independent injections of the SRM981 standard solution were treated with the traditionally used methods for isotope ratio calculation on transient signals; Point by Point (PbP), Linear Regression (LR) and Peak Area Integration (PAI). The results of the PbP and LR methods were compared before and after isotope ratio drift correction whereas with the PAI method only the no drift corrected data were treated. For the PAI method the integration of 100% of the peak area was selected and therefore time lag between the Faraday-amplifiers does not have any importance.

[0111] Epov et al. (Epov, V. N.; Rodriguez-Gonzalez, P.; Sonke, J. E.; Tessier, E.; Amouroux, D.; Bourgoin, L. M.; Donard, O. F. X. Analytical Chemistry 2008, 80, 3530-3538, Epov, V. N.; Berail, S.; Jimenez-Moreno, M.; Perrot, V.; Pecheyran, C.; Amouroux, D.; Donard, O. F. X. Analytical Chemistry 2010, 82, 5652-5662) found that the best isotope ratio precision using the PAI method obtained for an integration of 90-95% of the peak area. For the measured data, two different integration zones 95% and 100% of the peak area were tested and no significant differences were observed. 100% of the peak zone was also used for the LR method and the zone of the linear regression for the PbP method (Figure 6A, 6B and 6C, isotope ratio zone used for the linear regression). The blank intensity was calculated for each isotope as the average value of a zone (duration ~8 s) before the transient signal peak. The blank contribution was then subtracted from each intensity point of the respective isotopes. Isotope ratio drifts for all injections were corrected using Δt_{min} values obtained from the *Slope* model. The instrumental isotope mass fractionation was corrected internally using the $^{208}Pb/^{206}Pb$ ratio and the exponential mass fractionation low.

[0112] The blank-corrected and mass fractionation-corrected $^{207}Pb/^{206}Pb$, $^{204}Pb/^{206}Pb$ isotope ratios treated by different methods before and after isotope ratio drift correction are presented in Figure 8. Isotope ratio uncertainties for the PbP and LR methods were calculated for each individual injection by taking into account the uncertainties of the mass fractionation factor ($\beta_{208/206}$) and of the $^{207}Pb/^{206}Pb$, $^{204}Pb/^{206}Pb$ isotope ratios. The latters were calculated as the standard deviation (σ) for the PbP method and as the slope uncertainty (SE) for the LR method. The SE was calculated using the command *Regress* of *Mathematica* and can also be calculated using INDEX(LINEST(...)) function of MS EXCEL. Unlike PbP and LR methods, PAI method does not provide isotope ratio uncertainties for individual injections. All isotope ratio uncertainties are expressed for a coverage factor k=2.

[0113] As can be seen, for the PbP method both individual injection uncertainties and repeatability (σ of thirty injections) of the $^{204}Pb/^{206}Pb$, $^{207}Pb/^{206}Pb$ drift corrected ratios were surprisingly improved by a factor 20 and 13 respectively, compared to the results without drift correction. In contrast, for the isotope ratios treated with the LR method, repeatability before and after drift correction seems to be invariant but individual injection uncertainties were improved by a factor 14. Average values of $^{204}Pb/^{206}Pb$, $^{207}Pb/^{206}Pb$ individual injection uncertainties, repeatability and trueness are given in Table 3. As can be seen, contribution of the isotope ratio drift correction to individual injection uncertainty and to repeatability is most important for the ^{207}Pb/^{206}Pb ratio due certainly to higher drift compared to that of ^{204}Pb/^{206}Pb ratio. Drift correction has no statistically significant influence on the average trueness (trueness of the thirty measurements average); trueness variations are inferior to the measurement uncertainties, and therefore not significant (Table 3).

TABLE 1: MC-ICPMS and GC operating conditions and Faraday cup configuration

MC-ICPMS conditions			Neptune			Nu Plasma		
Sample Introduction System						GC		
Nebulizer			d-DIHEN			Microconcentric (for Tl)		
Spray chamber						Cinnabar 20 mL (for Tl)		
Sample gas			0.2 (L min^{-1})				20 (psi)	
Ar makeup gas (mL min^{-1})							0.4	
He GC carrier gas (mL min^{-1})							25	
Liquid uptake (μL min^{-1})			50			200 (for Tl)		
MC-ICPMS conditions								
RF power (W)			1200			1300		
Plasma gas flow rate (L min^{-1})			15			13		
Auxiliary flow rate (L min^{-1})			1.3			0.9		
Resolution			Low			Low		
Integration time (s)			0.262, 0.524, 1.049			0.5 (TRA mode)		
Sensitivity on ^{208}Pb (V ppm^{-1})			120			45		
Cup configuration	L3	L2	L1	Ax	H1	H2	H3	H4
Neptune	^{202}Hg		^{204}Pb		^{206}Pb	^{207}Pb	^{208}Pb	
Nu Plasma		^{202}Hg	^{203}Tl	^{204}Pb	^{205}Tl	^{206}Ph	^{207}Pb	^{208}Pb
Focus GC			*GC temp. Program*					
Injector			Split/splitless			Initial temperature (°C)		60
Injector volume (μL)			3			Initial time (min)		2
Injector Temperature (°C)			250			Ramp 1 (°C/min)		60
Column			MXT, 30 m, 0.53 mm i.d., 1.0 mm coating			Final temperature 1 (°C)		95
						Hold time (min)		5
						Ramp 2 (°C/min)		60
						Final temperature 2 (°C)		250
						Hold time (min)		1

TABLE 2: Direct injection - MC-ICPMS Δt_{min} values obtained by the *Slope* and *RSD* models for different integration times. The values of the slope and the %RSD calculated for the isotope ratios used for the linear regression were also presented.

(continued)

Int. Time (s)	$\Delta t_{\mu t v}$ (s)			Values of slope			Values of% RSD	
	Slope model	*RSD* model		No corrected	Corrected		No corrected	Corrected
0.262	0.00161	0.00151		1.14×10^{-4}	4.93×10^{-11}		0.0318	0.0208
0.524	0.00165	0.00154		8.95×10^{-5}	4.20×10^{-16}		0.0295	0.0197
1.049	0.00163	0.00157		8.33×10^{-5}	6.68×10^{-14}		0.0273	0.0132

TABLE 3: GC-MC-ICPMS average values of $^{207}Pb/^{206}Pb$ and $^{204}Pb/^{206}Pb$ isotope ratios uncertainty, repeatability and trueness of no corrected and corrected data for isotope ratio drift. Where PbP, LR and PAI are the Point by Point, the Linear Regression and the Peak Integration methods respectively. Uncertainties and repeat abilities are expressed for a coverage factor k=2.

$^{207}Pb/^{206}Pb$	**PbP**			**LR**			**PAI**
	No corrected	Corrected		No corrected	Corrected		No corrected
% Uncertainty	0.50	0.024		0.034	0.0024		
% Repeatability 0.098		0.0072		0.0062	0.0062		0.0058
% Trueness	0.030	0.014		0.018	0.019		0.016
$^{204}Pb/^{206}Pb$							
% Uncertainty	0.52	0.088		0.031	0.017		
% Repeatability	0.125	0.034		0.022	0.022		0.062
% Trueness	0.013	0.032		0.030	0.030		0.025

Claims

1. Method for correcting a drift of an isotopic ratio in a sample, on the basis of a first signal (I_a) and a second signal (I_b) derived from data measured by a multi-collector mass spectrometer, the first signal (I_a) representing a variation of a detected quantity of a first isotope (a) in the sample as a function of time, and the second signal (I_b) representing a variation of a detected quantity of a second isotope (b) in the sample as a function of time, said method comprising steps of:

   - applying (105) to the second signal (I_b) a time offset (Δt) so as to obtain a second offset signal ($I_b(t+\Delta t)$),
   - computing (106) values of isotopic ratio between the first signal (I_a) and the second offset signal ($I_b(t+\Delta t)$) at a plurality of times (t_i),
   - computing an isotopic ratio variation parameter as a function of the computed values of isotopic ratio,
   - adjusting the time offset (Δt) applied to the second signal (I_b) and repeating the preceding steps so as to determine a time offset (Δt_{min}) for which the isotopic ratio variation parameter is reduced.

2. Method according to claim 1, comprising a step of:

- computing the second signal ($I_b(t)$) by interpolation of second data representing detected quantities of a second isotope (b), measured in the sample at different times.

3. Method according to claim 2, wherein the interpolation is a piecewise polynomial interpolation.

4. Method according to one of claims 1 to 3, wherein the steps are applied to a number N of signals, N>2, each i-th signal representing a variation of a detected quantity of a i-th isotope in the sample as a function of time, so as to determine a time offset for each of the second to the N-th signals.

5. Method according to one of claims 1 to 4, wherein the isotopic ratio variation parameter is a slope of a straight line obtained by linear regression of the values of isotopic ratio.

6. Method according to one of claims 1 to 4, wherein the isotopic ratio variation parameter is a relative standard deviation of the values of isotopic ratio.

7. Method according to one of claims 1 to 6, comprising a step of:

- selecting a time interval in which the values of isotopic ratio are computed.

8. Method according to one of claims 1 to 6, wherein the steps are carried out on several time intervals, and a time offset is determined for each time interval.

9. Method according to one of claims 1 to 8, comprising preliminary steps of:

- introducing a sample into the multi-collector mass spectrometer, and
- measuring data from the sample, the data being measured by the spectrometer.

10. Method according to claim 9, wherein the multi-collector mass spectrometer is coupled to a separation system for separating the sample into several elementary fractions and successively introducing the elementary fractions into the spectrometer.

11. Method according to claim 10, wherein the separation system is a liquid, high performance liquid, ionic or a gas chromatography system.

12. Method according to claim 10, wherein the multi-collector mass spectrometer is coupled to a laser ablation system for in situ analysis of solid materials or single micrometric particle size analysis, so as to obtain the sample to be introduced into the multi-collector mass spectrometer.

13. Method according to one of claims 1 to 12, wherein the multi-collector mass spectrometer comprises an ion source selected from the group consisting in a thermal ionization device, an electron ionization device and a plasma ionization device.

14. Method according to one of claims 1 to 13, wherein the multi-collector mass spectrometer is a multi-collector inductively coupled plasma mass spectrometer.

15. Processing unit adapted for receiving data measured on a sample by a multi-collector mass spectrometer, and configured for correcting a drift of an isotopic ratio in the sample according to the method defined by one of claims 1 to 14.

16. Computer program for correcting a drift of an isotopic ratio in a sample from data measured on the sample by a multi-collector mass spectrometer, comprising program instructions for causing a processing unit to implement the method defined by one of claims 1 to 14.

FIG. 1

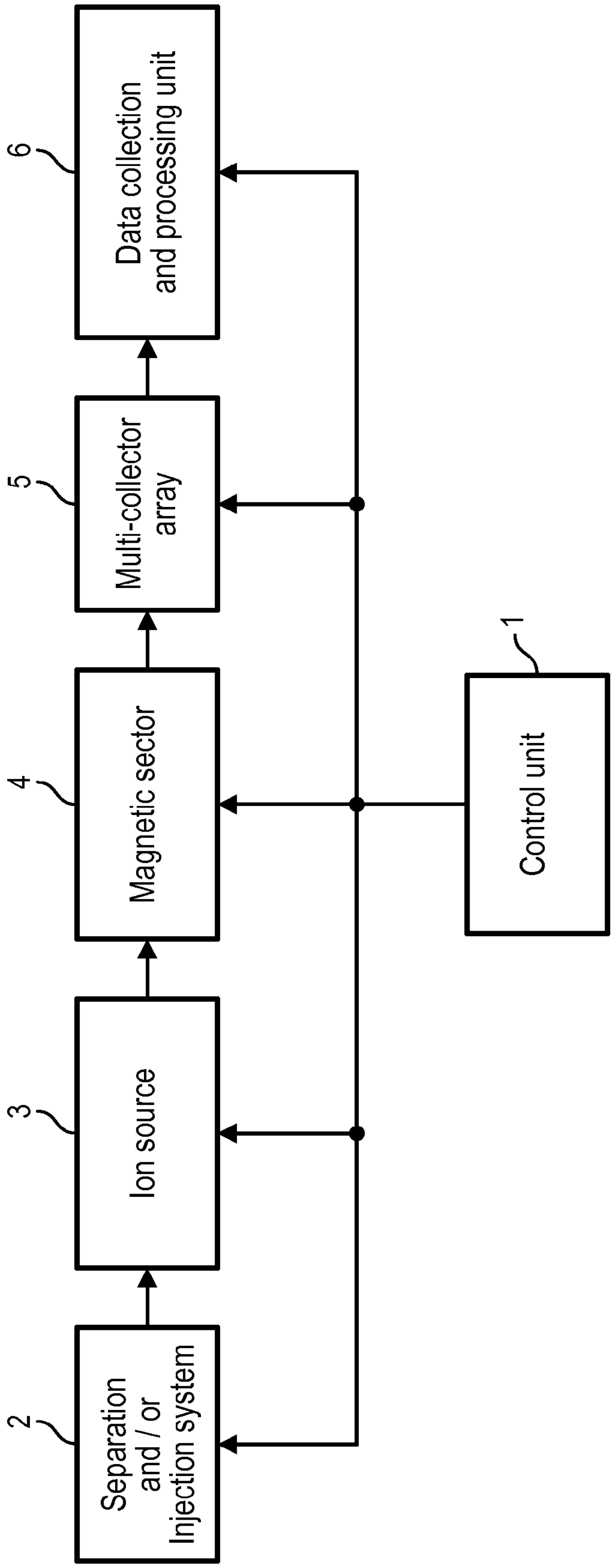
2
Separation and / or Injection system
3
Ion source
4
Magnetic sector
5
Multi-collector array
6
Data collection and processing unit
1
Control unit

FIG. 2

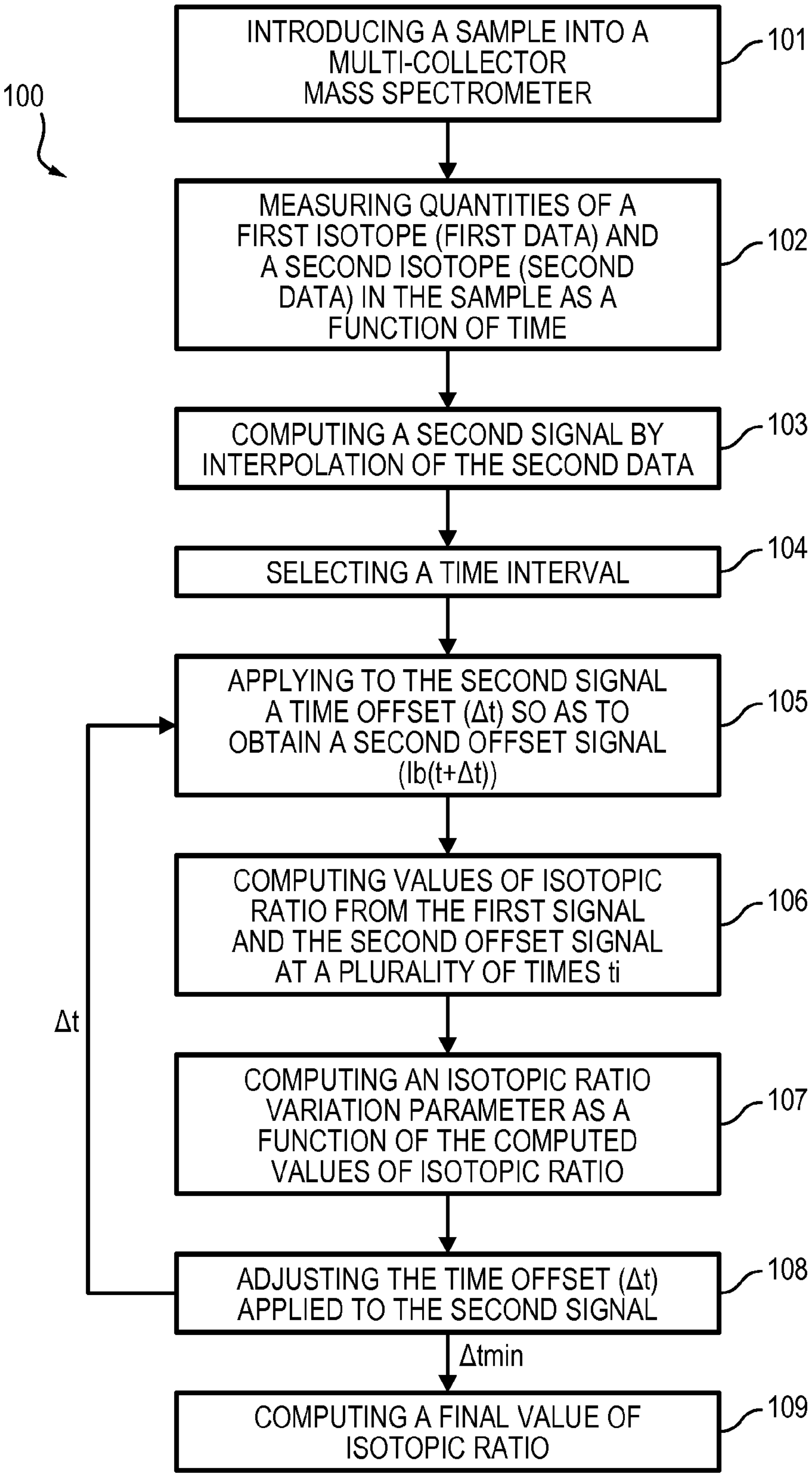
100
INTRODUCING A SAMPLE INTO A MULTI-COLLECTOR MASS SPECTROMETER
101
MEASURING QUANTITIES OF A FIRST ISOTOPE (FIRST DATA) AND A SECOND ISOTOPE (SECOND DATA) IN THE SAMPLE AS A FUNCTION OF TIME
102
COMPUTING A SECOND SIGNAL BY INTERPOLATION OF THE SECOND DATA
103
SELECTING A TIME INTERVAL
104
APPLYING TO THE SECOND SIGNAL A TIME OFFSET (Δt) SO AS TO OBTAIN A SECOND OFFSET SIGNAL (Ib(t+Δt))
105
COMPUTING VALUES OF ISOTOPIC RATIO FROM THE FIRST SIGNAL AND THE SECOND OFFSET SIGNAL AT A PLURALITY OF TIMES ti
106
Δt
COMPUTING AN ISOTOPIC RATIO VARIATION PARAMETER AS A FUNCTION OF THE COMPUTED VALUES OF ISOTOPIC RATIO
107
ADJUSTING THE TIME OFFSET (Δt) APPLIED TO THE SECOND SIGNAL
108
Δtmin
COMPUTING A FINAL VALUE OF ISOTOPIC RATIO
109

FIG. 3A

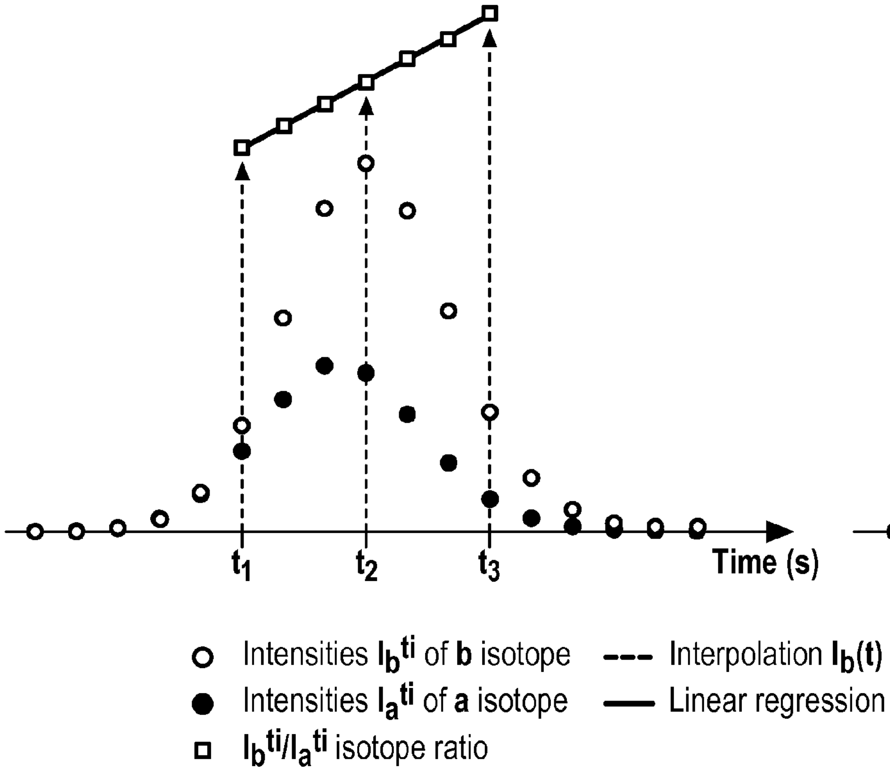
t1
t2
t3
Time (s)
○ Intensities I_b^{ti} of b isotope
● Intensities I_a^{ti} of a isotope
□ I_b^{ti}/I_a^{ti} isotope ratio
--- Interpolation $I_b(t)$
— Linear regression

FIG. 3B

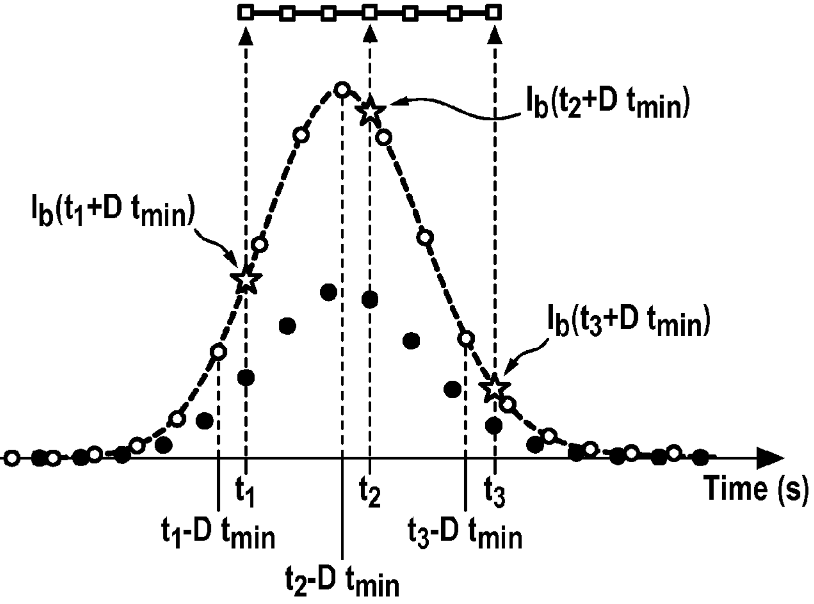
$I_b(t_1+D\ t_{min})$
$I_b(t_2+D\ t_{min})$
$I_b(t_3+D\ t_{min})$
t1
t2
t3
t_1-D t_{min}
t_2-D t_{min}
t_3-D t_{min}
Time (s)

FIG. 4A

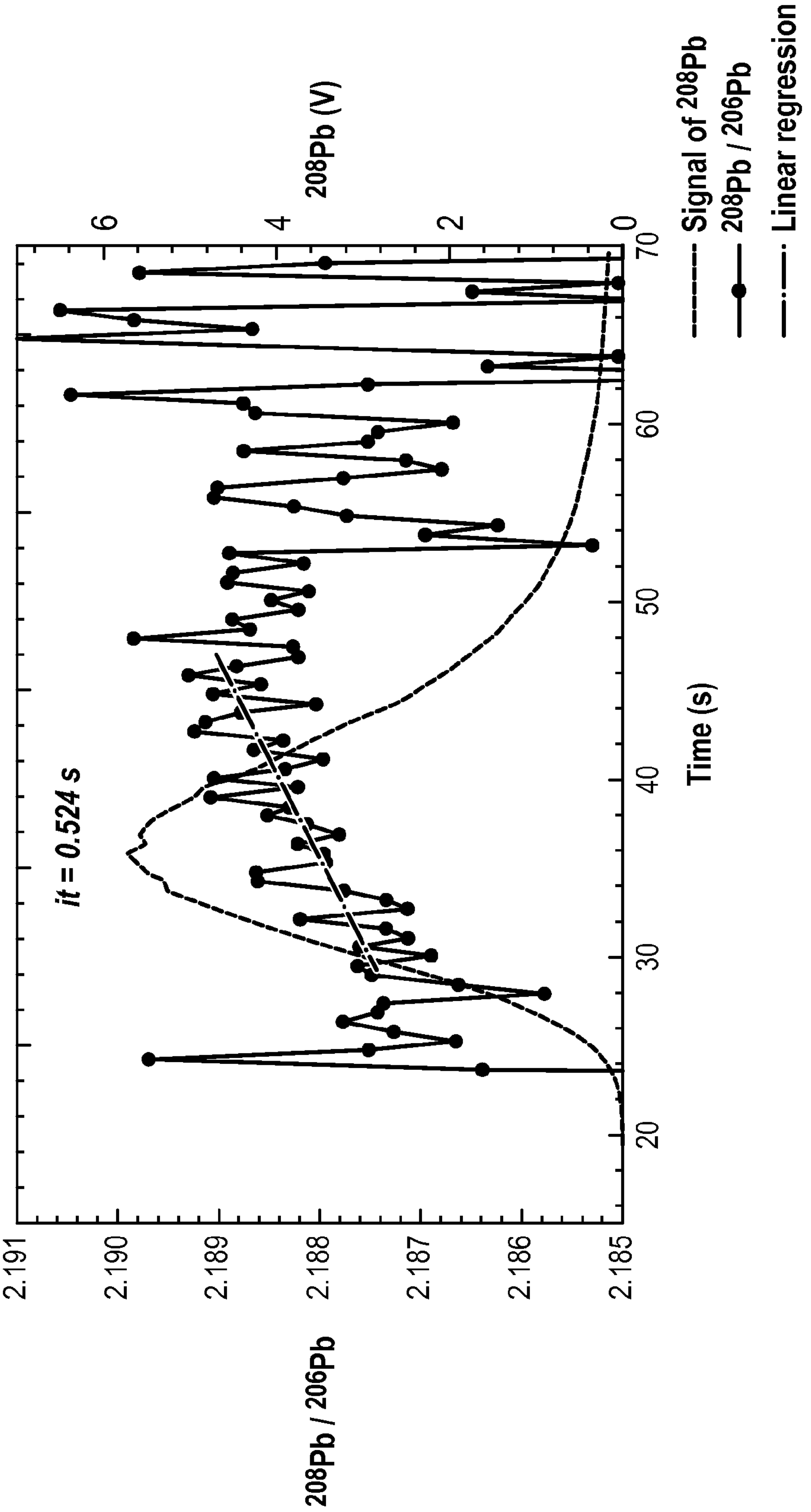
it = 0.524 s
208Pb / 206Pb
2.191
2.190
2.189
2.188
2.187
2.186
2.185
208Pb (V)
6
4
2
0
20
30
40
50
60
70
Time (s)
Signal of 208Pb
208Pb / 206Pb
Linear regression

FIG. 4B

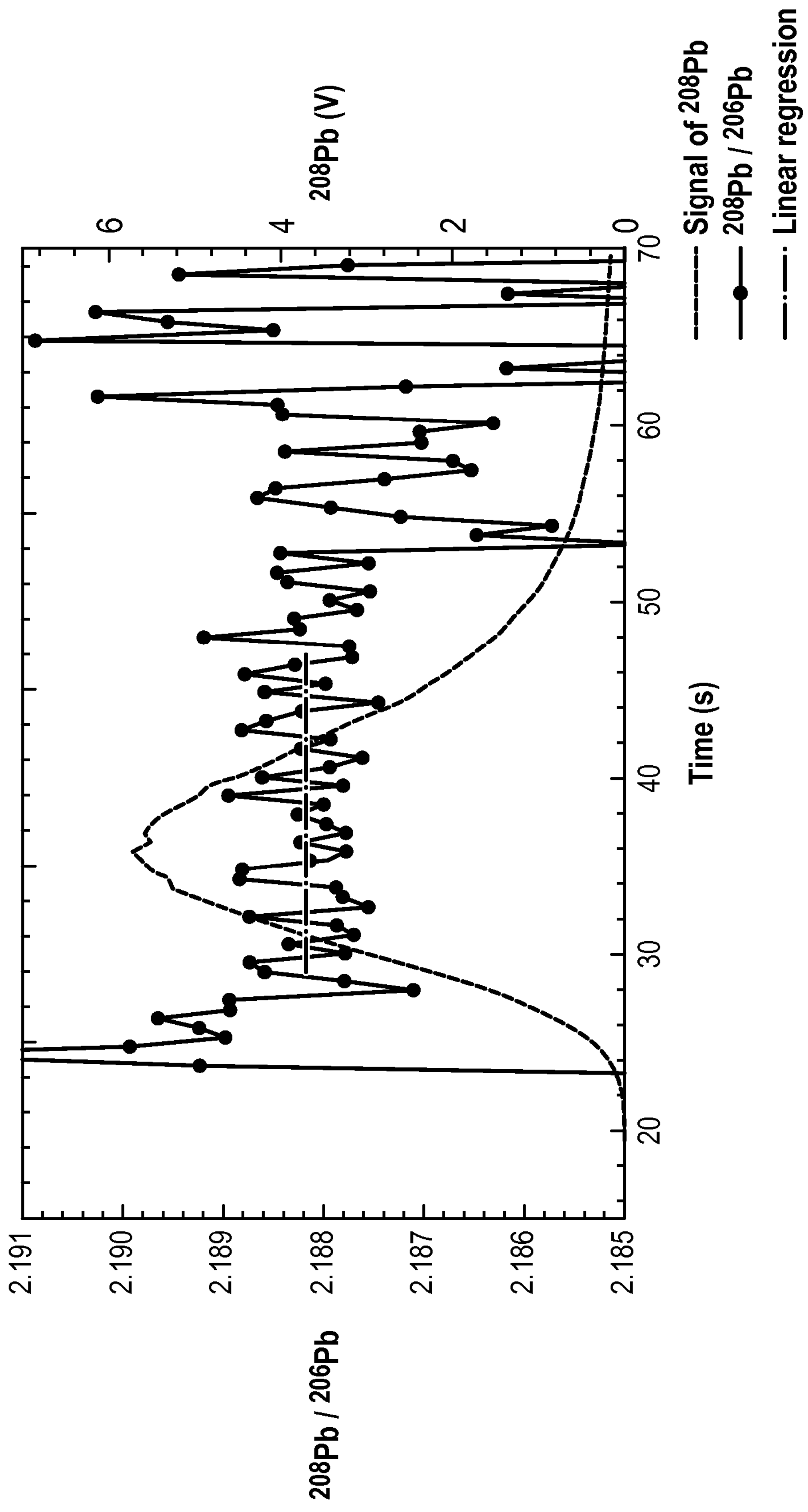
^{208}Pb / ^{206}Pb
2.191
2.190
2.189
2.188
2.187
2.186
2.185
^{208}Pb (V)
6
4
2
0
20
30
40
50
60
70
Time (s)
Signal of ^{208}Pb
^{208}Pb / ^{206}Pb
Linear regression

FIG. 4C

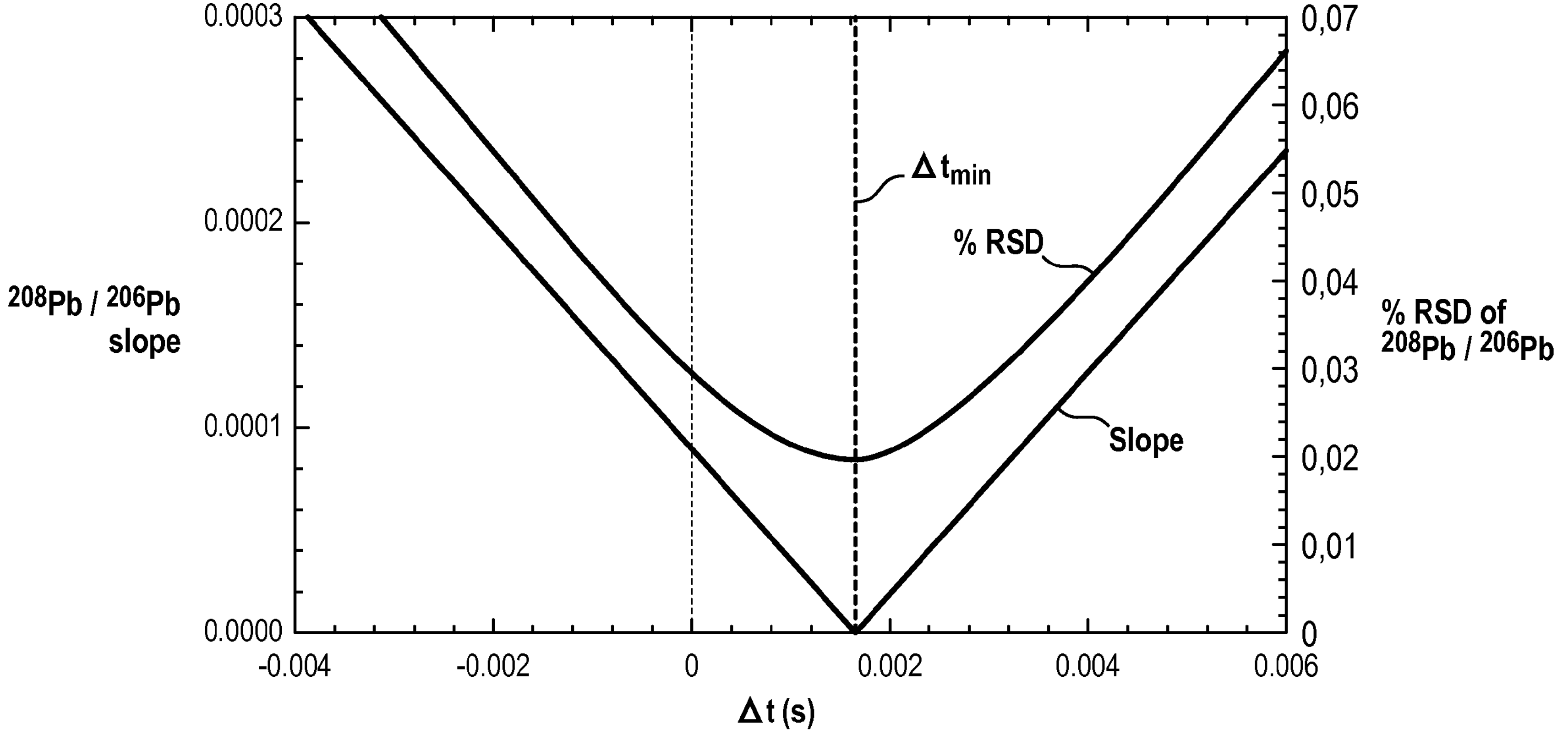
0.0003
0.0002
0.0001
0.0000
208Pb / 206Pb slope
0,07
0,06
0,05
0,04
0,03
0,02
0,01
0
% RSD of 208Pb / 206Pb
-0.004
-0.002
0
0.002
0.004
0.006
Δt (s)
Δtmin
% RSD
Slope

FIG. 5A

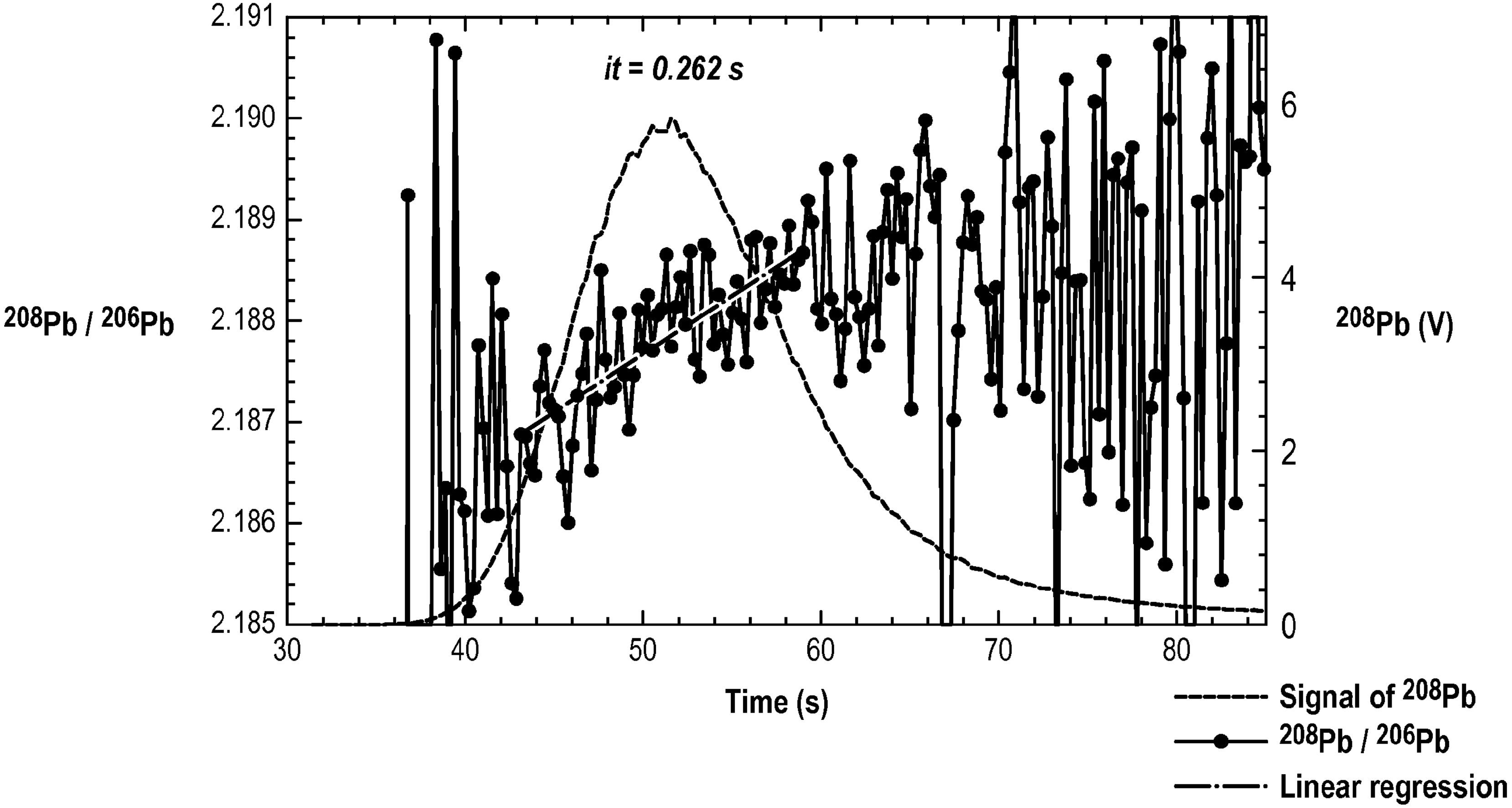
it = 0.262 s
^{208}Pb / ^{206}Pb
2.191
2.190
2.189
2.188
2.187
2.186
2.185
^{208}Pb (V)
6
4
2
0
30
40
50
60
70
80
Time (s)
Signal of ^{208}Pb
^{208}Pb / ^{206}Pb
Linear regression

FIG. 5B

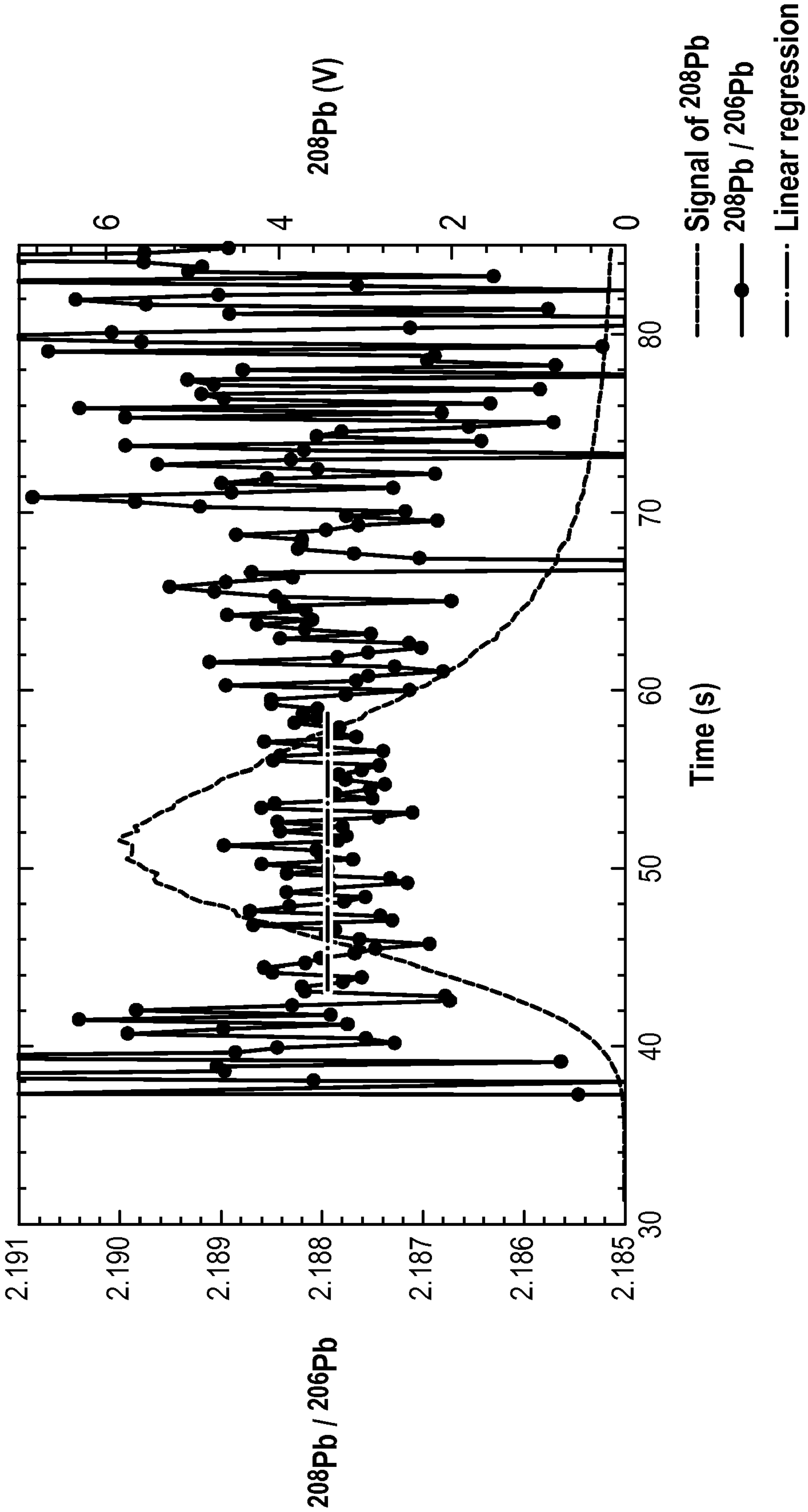
208Pb / 206Pb
2.191
2.190
2.189
2.188
2.187
2.186
2.185
208Pb (V)
6
4
2
0
30
40
50
60
70
80
Time (s)
Signal of 208Pb
208Pb / 206Pb
Linear regression

FIG. 5C

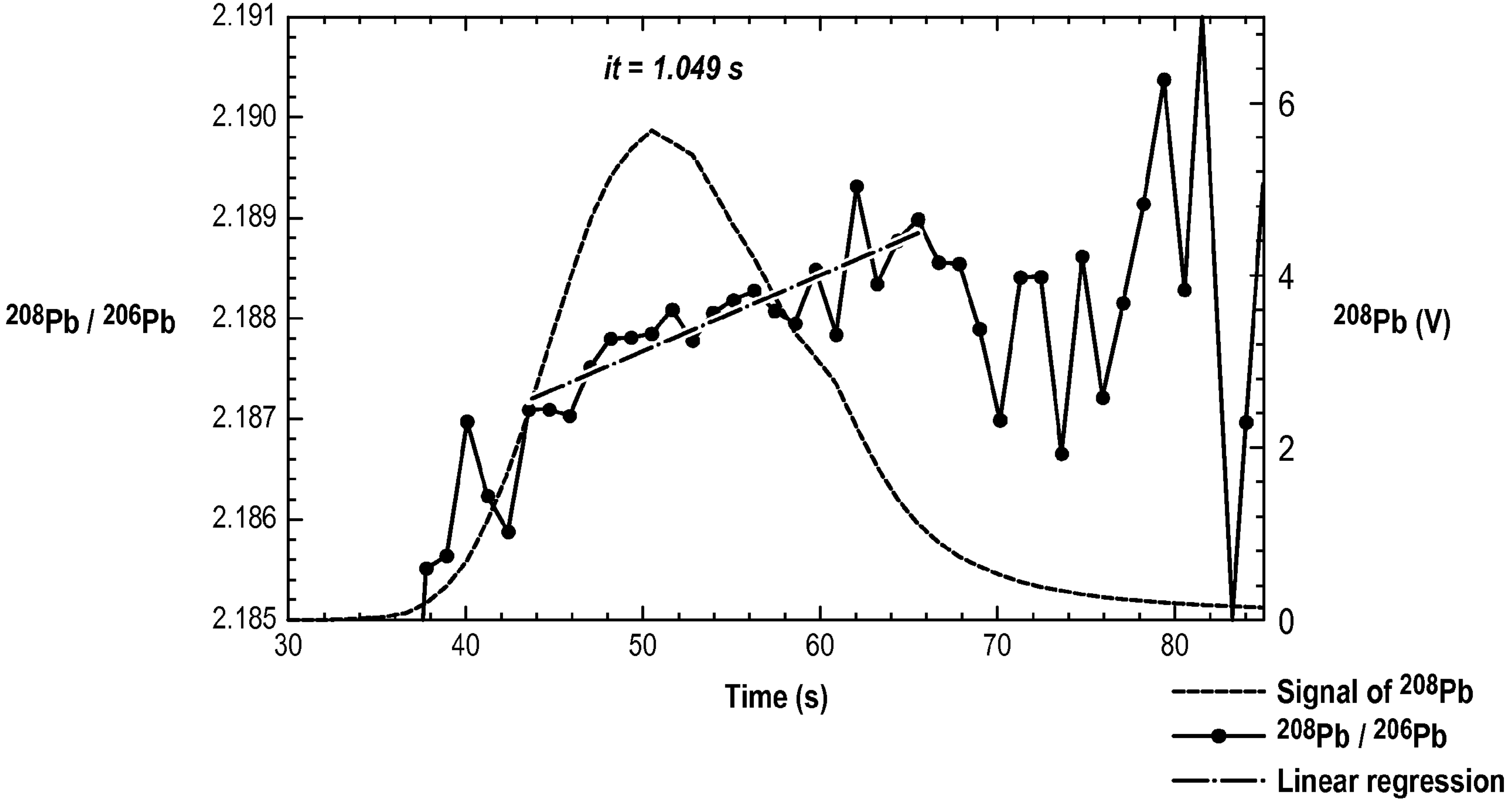
it = 1.049 s
^{208}Pb / ^{206}Pb
2.191
2.190
2.189
2.188
2.187
2.186
2.185
^{208}Pb (V)
6
4
2
0
30
40
50
60
70
80
Time (s)
Signal of ^{208}Pb
^{208}Pb / ^{206}Pb
Linear regression

FIG. 5D

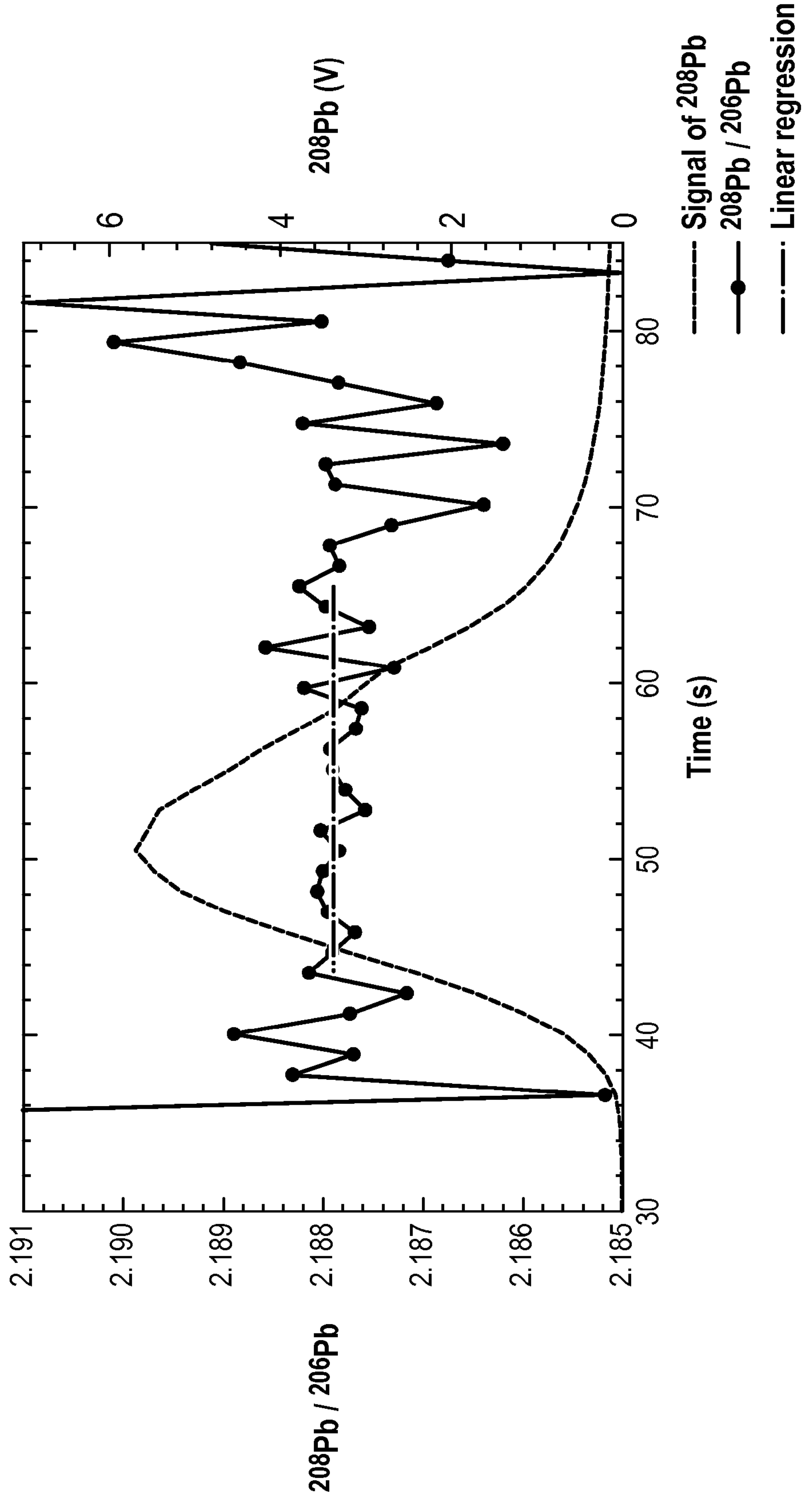
208Pb / 206Pb
2.191
2.190
2.189
2.188
2.187
2.186
2.185
208Pb (V)
6
4
2
0
Time (s)
30
40
50
60
70
80
Signal of 208Pb
208Pb / 206Pb
Linear regression

FIG. 6A

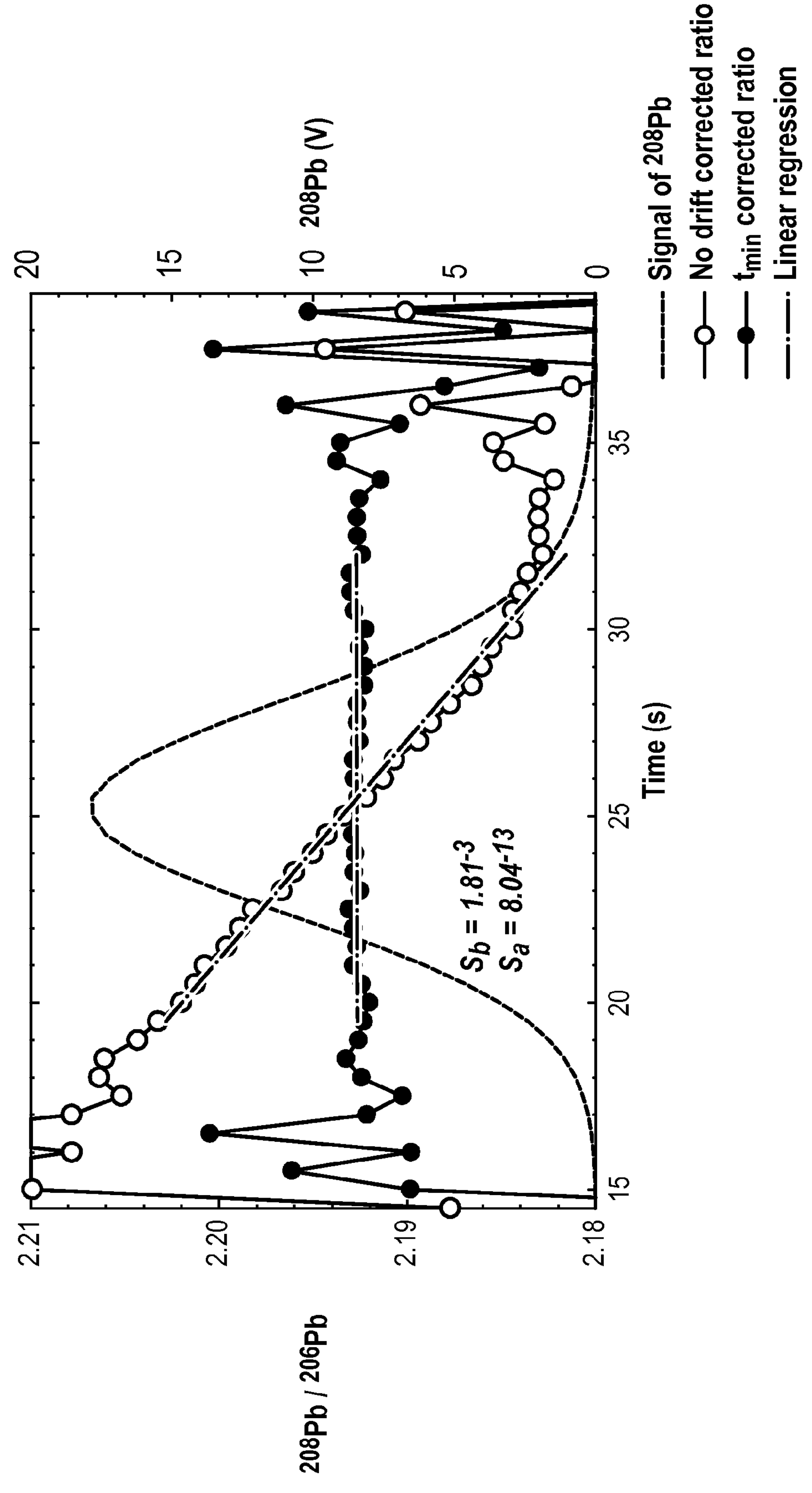
208Pb / 206Pb
2.21
2.20
2.19
2.18
208Pb (V)
20
15
10
5
0
15
20
25
30
35
Time (s)
$S_b = 1.81^{-3}$
$S_a = 8.04^{-13}$
Signal of 208Pb
No drift corrected ratio
t_{min} corrected ratio
Linear regression

FIG. 6B

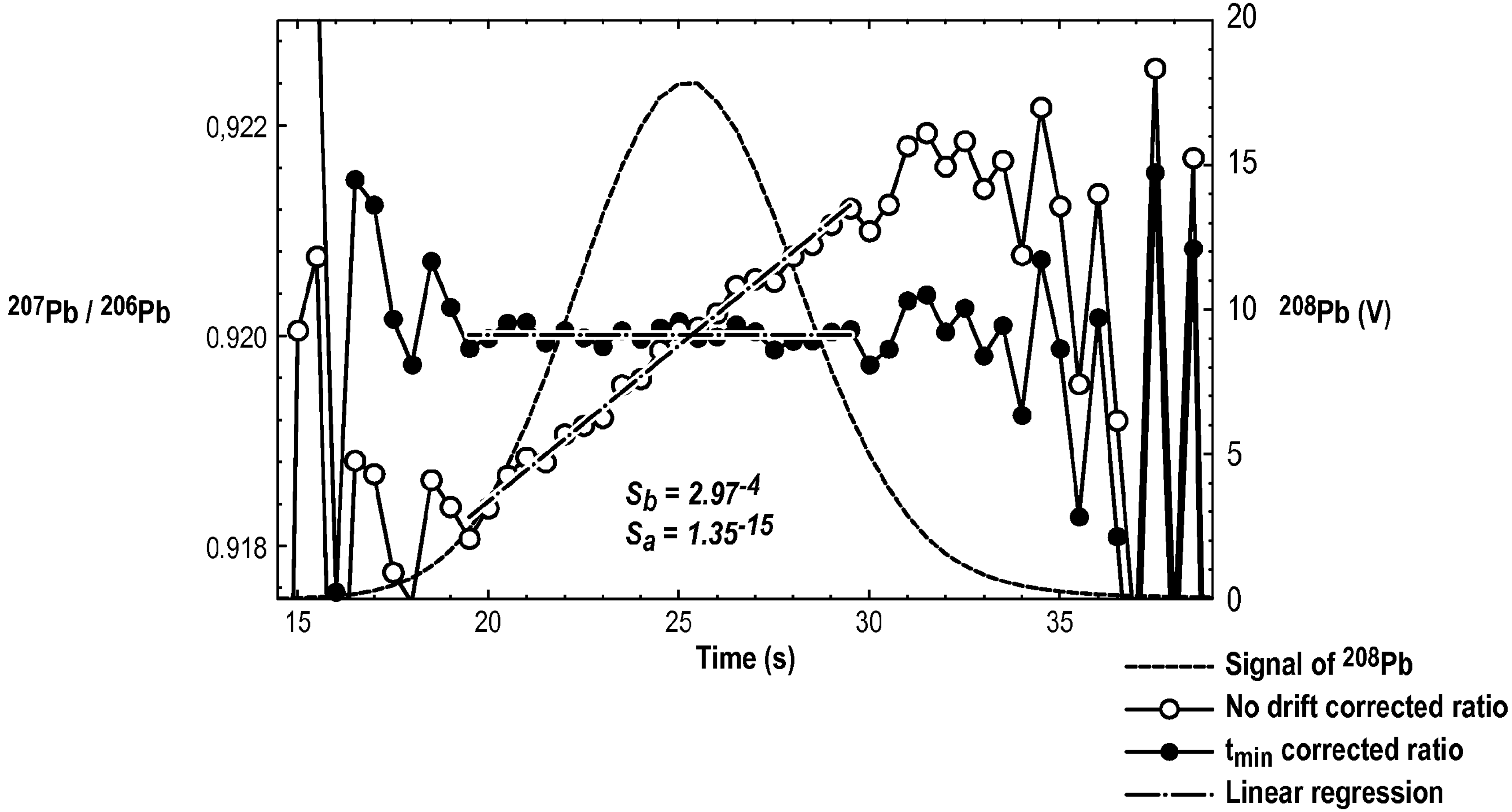
^{207}Pb / ^{206}Pb
0,922
0.920
0.918
20
15
10
5
0
^{208}Pb (V)
15
20
25
30
35
Time (s)
$S_b = 2.97^{-4}$
$S_a = 1.35^{-15}$
Signal of ^{208}Pb
No drift corrected ratio
t_{min} corrected ratio
Linear regression

FIG. 6C

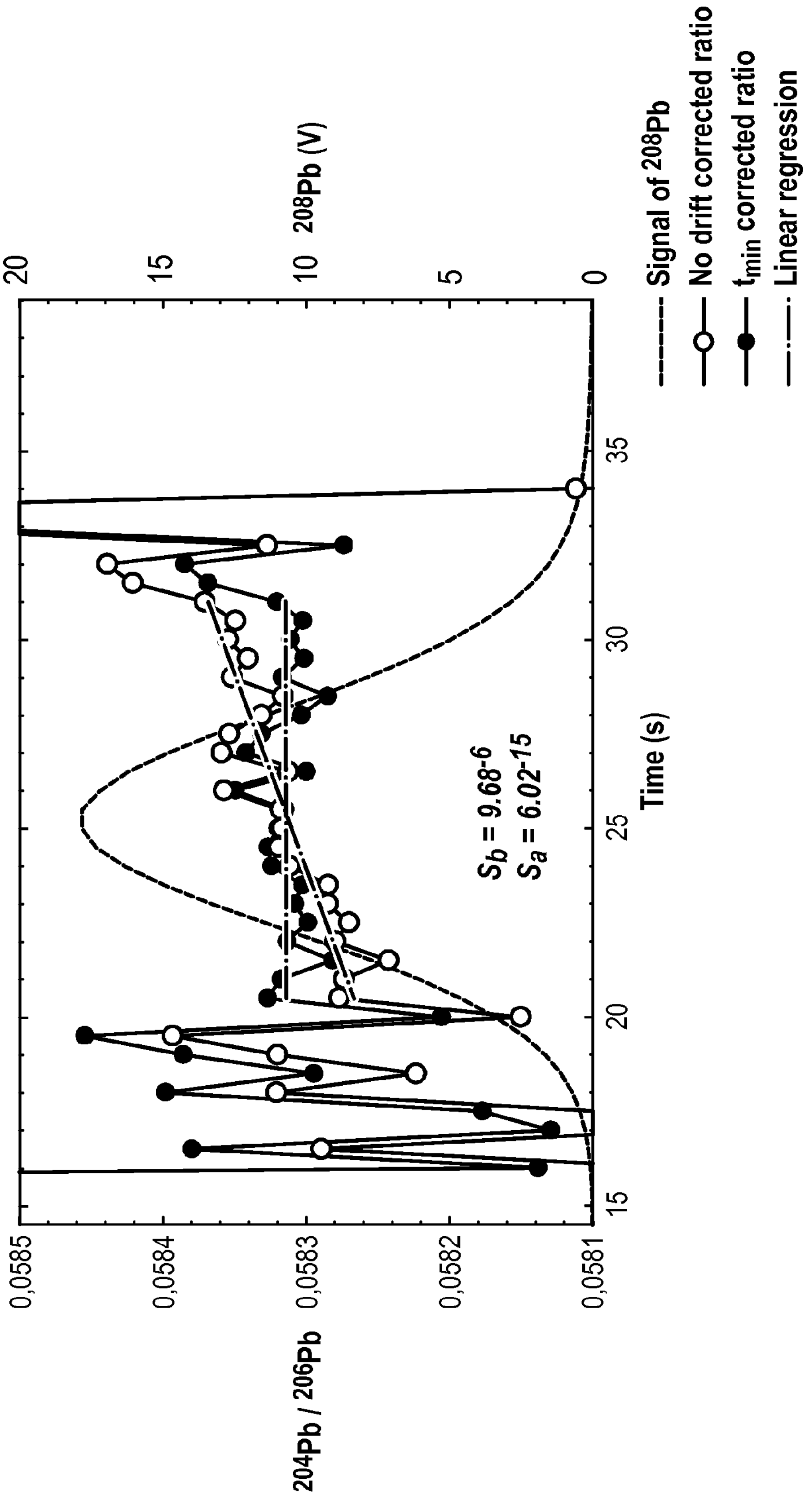
204Pb / 206Pb
0,0581
0,0582
0,0583
0,0584
0,0585
208Pb (V)
0
5
10
15
20
Time (s)
15
20
25
30
35
$S_b = 9.68^{-6}$
$S_a = 6.02^{-15}$
Signal of ^{208}Pb
No drift corrected ratio
t_{min} corrected ratio
Linear regression

FIG. 6D

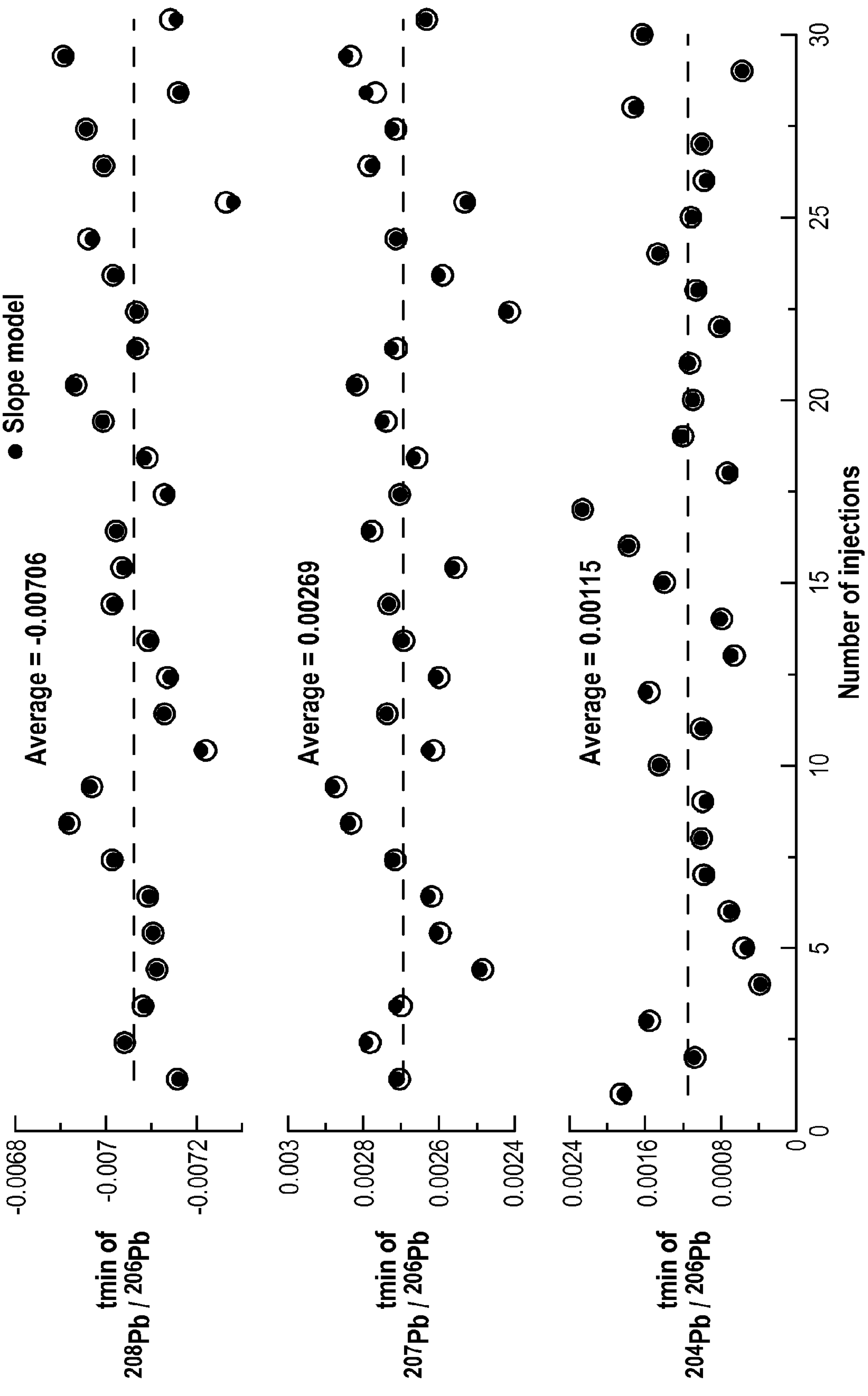
○ RSD Model
● Slope model
Average = -0.00706
Average = 0.00269
Average = 0.00115
tmin of 208Pb / 206Pb
tmin of 207Pb / 206Pb
tmin of 204Pb / 206Pb
-0.0068
-0.007
-0.0072
0.003
0.0028
0.0026
0.0024
0.0024
0.0016
0.0008
0
0
5
10
15
20
25
30
Number of injections

FIG. 7A

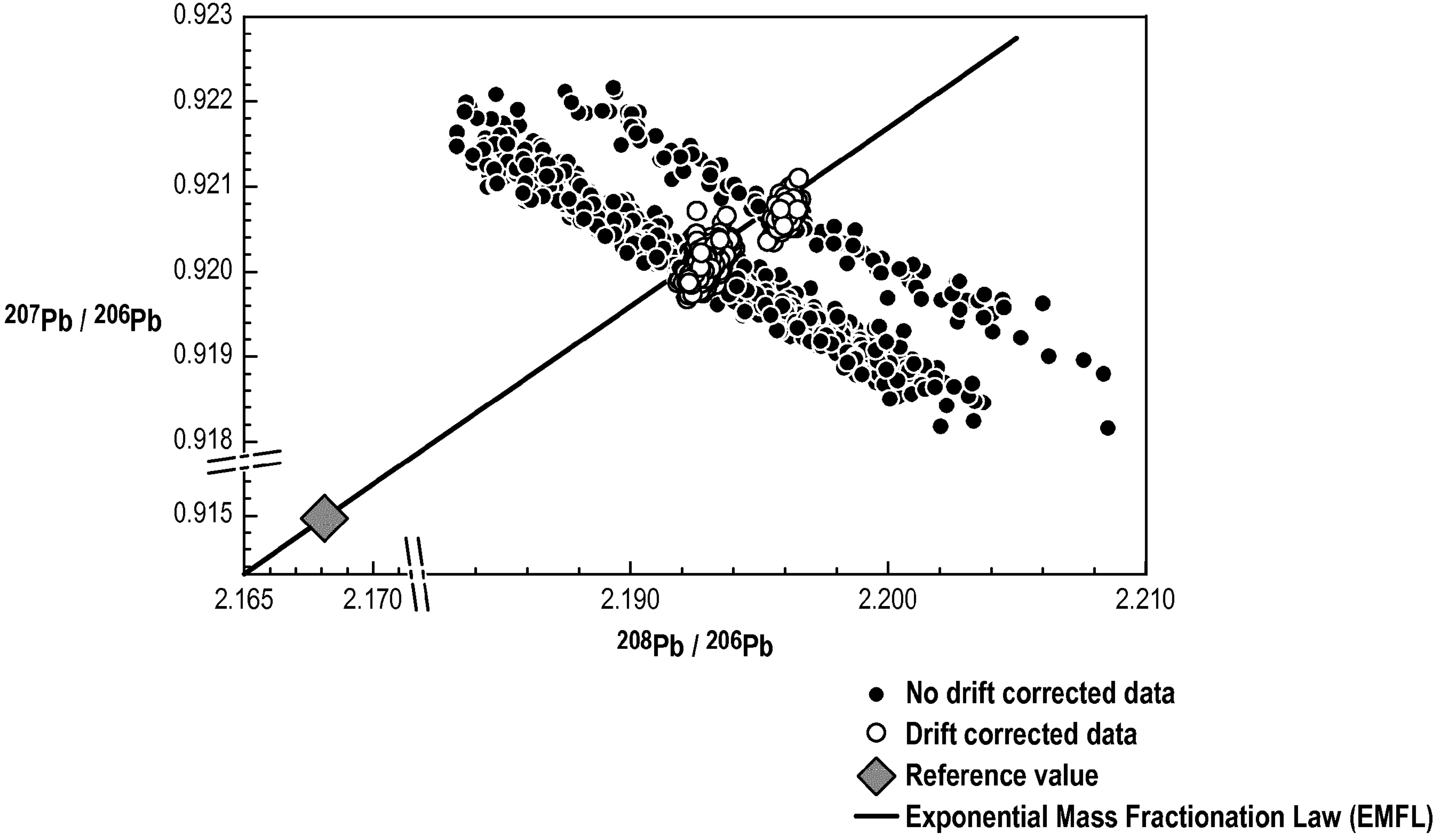
^{207}Pb / ^{206}Pb
0.923
0.922
0.921
0.920
0.919
0.918
0.915
2.165
2.170
2.190
2.200
2.210
^{208}Pb / ^{206}Pb
● No drift corrected data
○ Drift corrected data
◆ Reference value
— Exponential Mass Fractionation Law (EMFL)

FIG. 7B

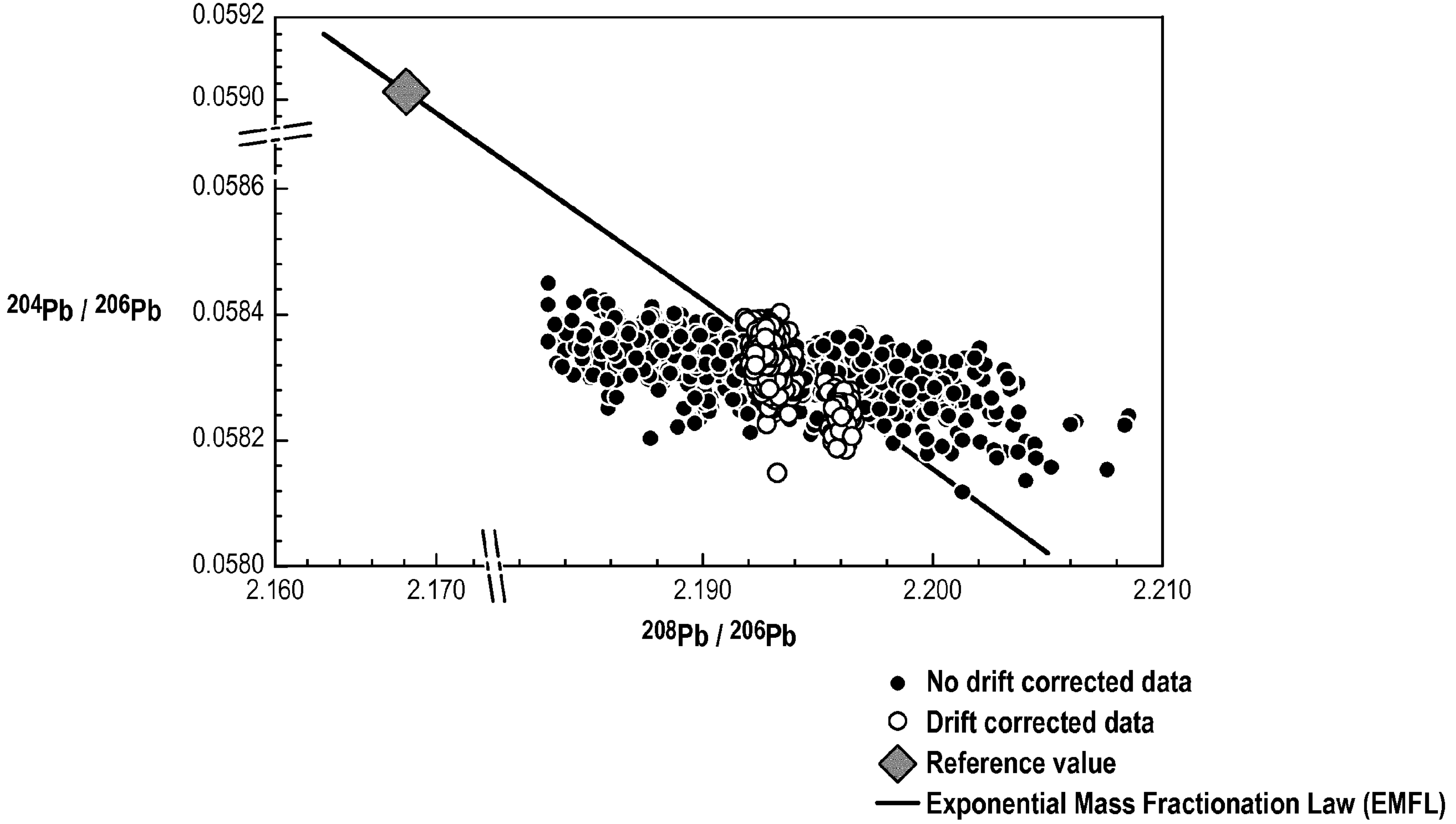
0.0592
0.0590
0.0586
0.0584
0.0582
0.0580
^{204}Pb / ^{206}Pb
2.160
2.170
2.190
2.200
2.210
^{208}Pb / ^{206}Pb
● No drift corrected data
○ Drift corrected data
Reference value
Exponential Mass Fractionation Law (EMFL)

FIG. 7C

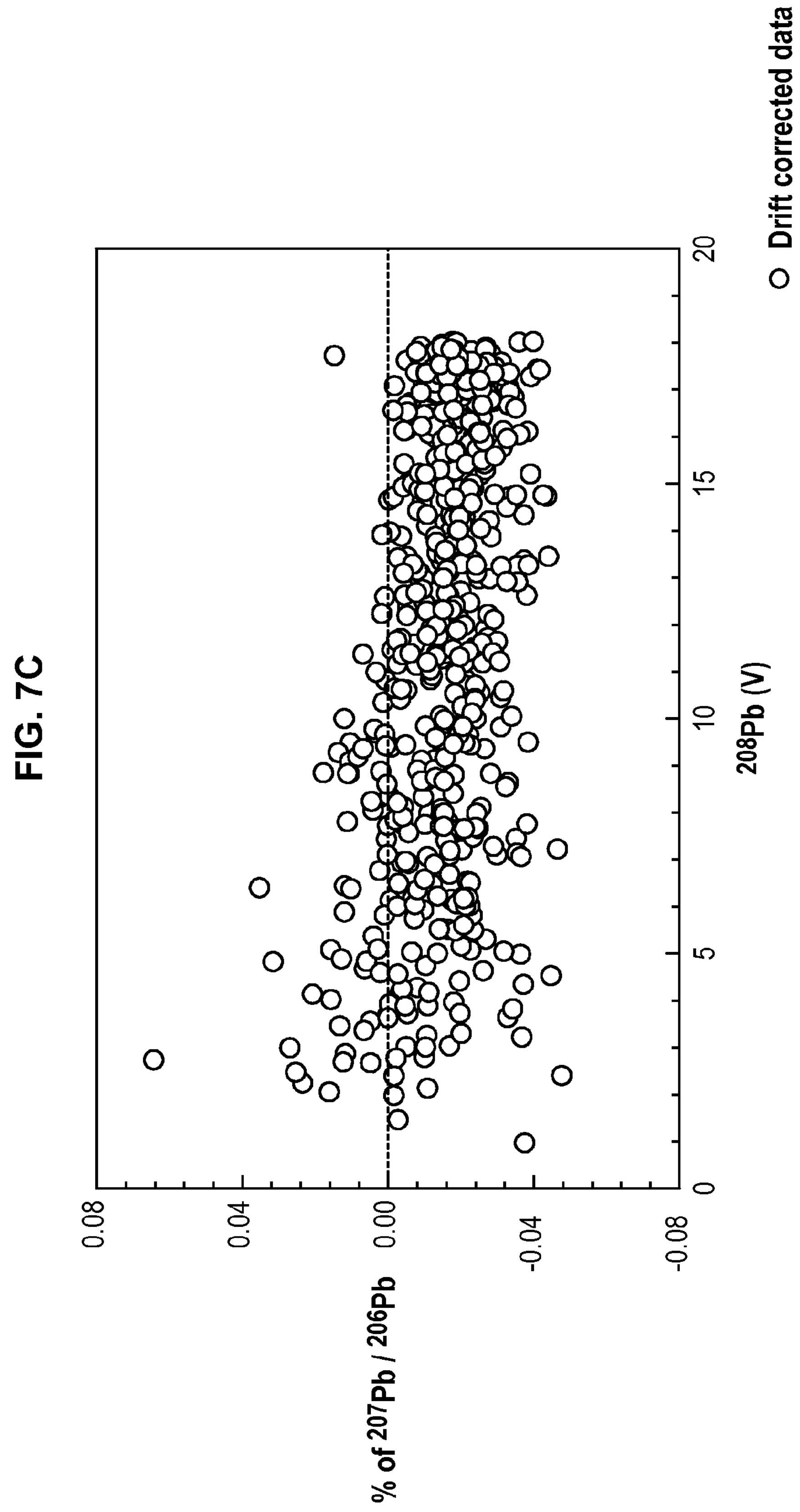
% of 207Pb / 206Pb
0.08
0.04
0.00
-0.04
-0.08
0
5
10
15
20
208Pb (V)
Drift corrected data

FIG. 7D

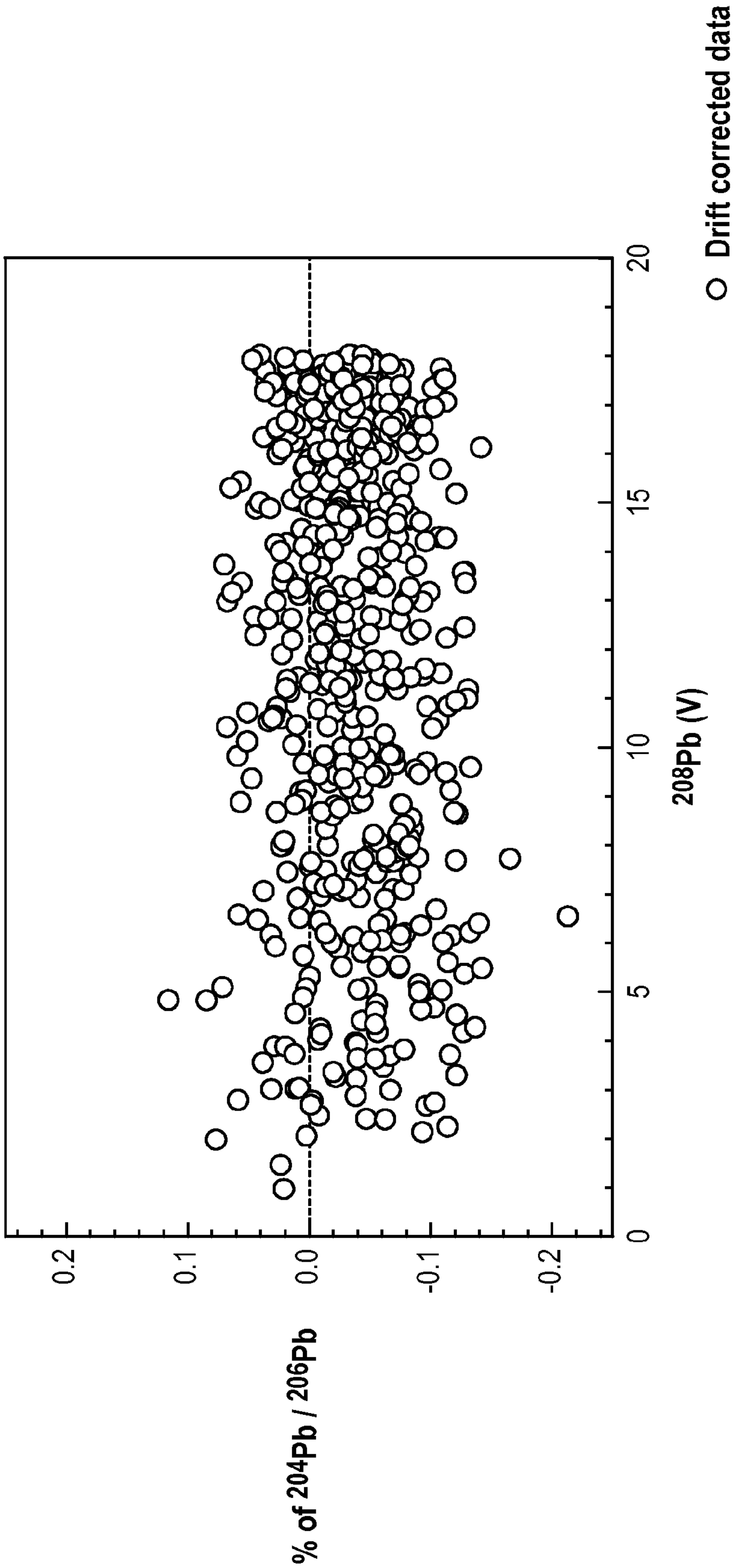
% of ^{204}Pb / ^{206}Pb
0.2
0.1
0.0
-0.1
-0.2
0
5
10
15
20
^{208}Pb (V)
○ Drift corrected data

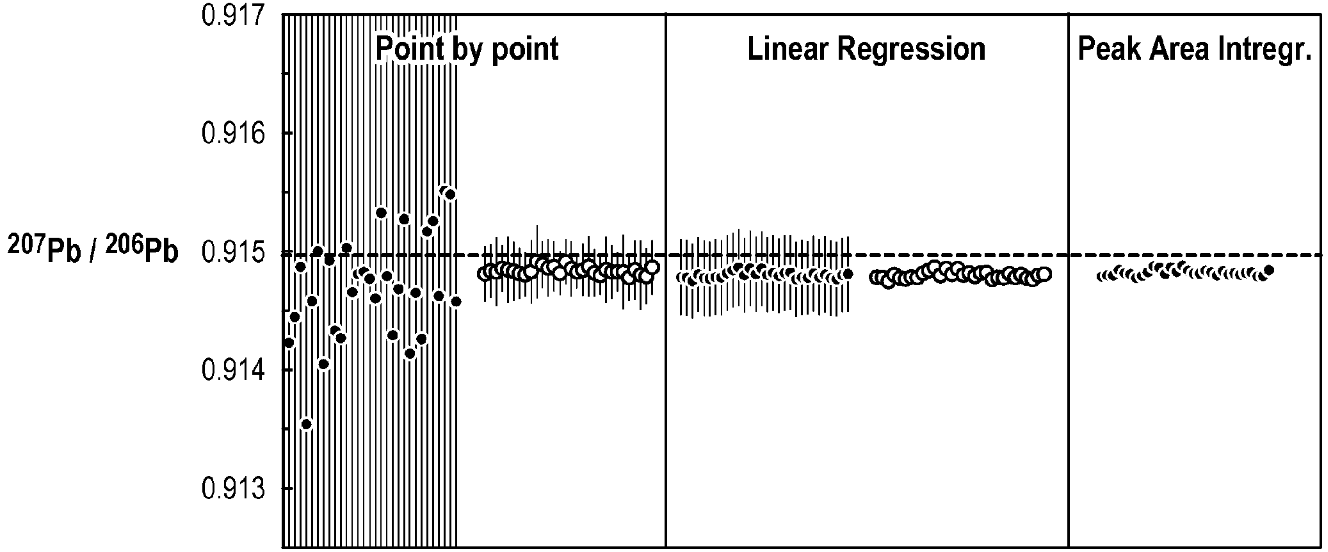
0.917
0.916
0.915
0.914
0.913
^{207}Pb / ^{206}Pb
Point by point
Linear Regression
Peak Area Intregr.

FIG. 8A

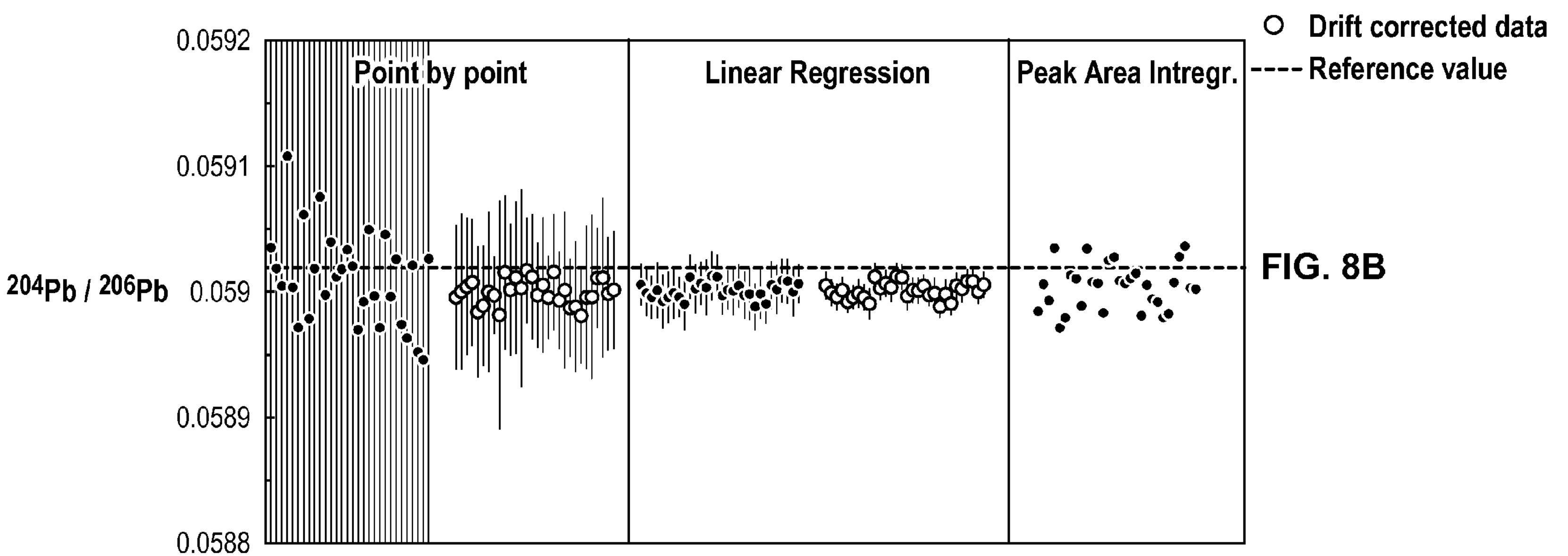
0.0592
0.0591
0.059
0.0589
0.0588
^{204}Pb / ^{206}Pb
Point by point
Linear Regression
Peak Area Intregr.
● No drift corrected data
○ Drift corrected data
---- Reference value

FIG. 8B

Europäisches Patentamt
European Patent Office
Office européen des brevets

EUROPEAN SEARCH REPORT

Application Number
EP 13 30 6552

DOCUMENTS CONSIDERED TO BE RELEVANT

Category	Citation of document with indication, where appropriate, of relevant passages	Relevant to claim	CLASSIFICATION OF THE APPLICATION (IPC)
A	THOMAS PETTKE ET AL: "Quantification of transient signals in multiple collector inductively coupled plasma mass spectrometry: accurate lead isotope ratio determination by laser ablation of individual fluid inclusions", JOURNAL OF ANALYTICAL ATOMIC SPECTROMETRY, vol. 26, no. 3, 1 January 2011 (2011-01-01), page 475, XP055122636, ISSN: 0267-9477, DOI: 10.1039/c0ja00140f * page 481 - page 484; figures 4,5 * -----	1-16	INV. H01J49/00
A,D	VLADIMIR N. EPOV ET AL: "Simultaneous Determination of Species-Specific Isotopic Composition of Hg by Gas Chromatography Coupled to Multicollector ICPMS", ANALYTICAL CHEMISTRY, vol. 80, no. 10, 1 May 2008 (2008-05-01), pages 3530-3538, XP055122067, ISSN: 0003-2700, DOI: 10.1021/ac800384b * abstract * * page 3534 - page 3535; figures 3-5 * -----	1-16	TECHNICAL FIELDS SEARCHED (IPC) H01J
A	EHRLICH S ET AL: "Experimental study of the copper isotope fractionation between aqueous Cu(II) and covellite, CuS", CHEMICAL GEOLOGY, ELSEVIER SCIENCE PUBLISHER B.V., AMSTERDAM, NL, vol. 209, no. 3-4, 27 September 2004 (2004-09-27), pages 259-269, XP004549123, ISSN: 0009-2541, DOI: 10.1016/J.CHEMGEO.2004.06.010 * page 263 - page 264; figure 2 * ----- -/--	1	

The present search report has been drawn up for all claims

Place of search	Date of completion of the search	Examiner
The Hague	12 June 2014	Loiseleur, Pierre

CATEGORY OF CITED DOCUMENTS

X : particularly relevant if taken alone
Y : particularly relevant if combined with another document of the same category
A : technological background
O : non-written disclosure
P : intermediate document

T : theory or principle underlying the invention
E : earlier patent document, but published on, or after the filing date
D : document cited in the application
L : document cited for other reasons
& : member of the same patent family, corresponding document

1

EPO FORM 1503 03.82 (P04C01)

Europäisches
Patentamt
European
Patent Office
Office européen
des brevets

EUROPEAN SEARCH REPORT

Application Number
EP 13 30 6552

DOCUMENTS CONSIDERED TO BE RELEVANT

Category	Citation of document with indication, where appropriate, of relevant passages	Relevant to claim	CLASSIFICATION OF THE APPLICATION (IPC)
A	COAKLEY K J ET AL: "Secondary ion mass spectrometry measurements of isotopic ratios: correction for time varying count rate", INTERNATIONAL JOURNAL OF MASS SPECTROMETRY, ELSEVIER SCIENCE PUBLISHERS, AMSTERDAM, NL, vol. 240, no. 2, 15 January 2005 (2005-01-15), pages 107-120, XP027705160, ISSN: 1387-3806 [retrieved on 2005-01-15] * the whole document * -----	1	
			TECHNICAL FIELDS SEARCHED (IPC)

The present search report has been drawn up for all claims

1

Place of search	Date of completion of the search	Examiner
The Hague	12 June 2014	Loiseleur, Pierre

CATEGORY OF CITED DOCUMENTS

X : particularly relevant if taken alone
Y : particularly relevant if combined with another document of the same category
A : technological background
O : non-written disclosure
P : intermediate document

T : theory or principle underlying the invention
E : earlier patent document, but published on, or after the filing date
D : document cited in the application
L : document cited for other reasons
....
& : member of the same patent family, corresponding document

EPO FORM 1503 03.82 (P04C01)

REFERENCES CITED IN THE DESCRIPTION

Non-patent literature cited in the description

- **DOUCELANCE, R. ; MANHÈS, G.** *Chemical Geology,* 2001, vol. 176, 361-377 **[0089]**
- **EPOV, V. N. ; RODRIGUEZ-GONZALEZ, P. ; SONKE, J. E. ; TESSIER, E. ; AMOUROUX, D.; ; BOURGOIN, L. M. ; DONARD, O. F. X.** *Analytical Chemistry,* 2008, vol. 80, 3530-3538 **[0111]**
- **EPOV, V. N. ; JIMENEZ-MORENO, M. ; PERROT, V. ; PECHEYRAN, C ; AMOUROUX, D. ; DONARD, O. F. X.** *Analytical Chemistry,* vol. 82, 5652-5662 **[0111]**